

Figure 3. Effects of DCA on CHF rats. A, Administration of DCA or vehicle to DS rats with LVH started from 11 weeks (W) of age. DCA improved the survival of CHF rats. B, Representative images of echocardiography, showing that DCA improved systolic cardiac function. C, DCA attenuated the increase in the plasma concentrations of brain natriuretic peptides at the CHF stage. D, CHF rats showed increased heart weight and lung weight per body weight, and DCA ameliorated the increase. E, PDH activity was unchanged at the LVH or CHF stage and was increased by DCA. Representative images and quantification by densitometry. The mean value for control rats was expressed as 1 unit. F, Plasma lactate and pyruvate levels. * $P < 0.05$ vs control rats with vehicle or DCA. † $P < 0.05$ vs vehicle-treated rats on the same diet. $n = 5-8$ for each group.

DCA Prevented the Transition From LVH to CHF

To test whether the modulation of cardiac energy metabolism prevents the transition from cardiac hypertrophy to heart failure, the effect of DCA was examined. Long-term administration of DCA starting at 11 weeks of age improved the survival of DS rats that were fed an HS diet (Figure 3A). On echocardiographic examination, DCA preserved systolic function as assessed by fractional shortening (Figure 3B and supplemental Table II). DCA decreased plasma levels of brain natriuretic peptides at the CHF stage (Figure 3C). DCA

ameliorated the increase in heart and lung weights of CHF rats (Figure 3D and supplemental Table V). DCA attenuated the fibrosis of the myocardium in CHF rats (supplemental Figure IIA and IIB). Very few apoptotic cells were observed in heart tissues of CHF rats, with no difference compared with control rats (supplemental Figure IIC and IID). Thus, DCA preserved cardiac function and prevented CHF. PDH activity in heart tissue was unchanged at the LVH or CHF stage but was increased by DCA (Figure 3E). DCA increased PDH activity in cardiomyocytes (supplemental Figure III). Plasma lactate level

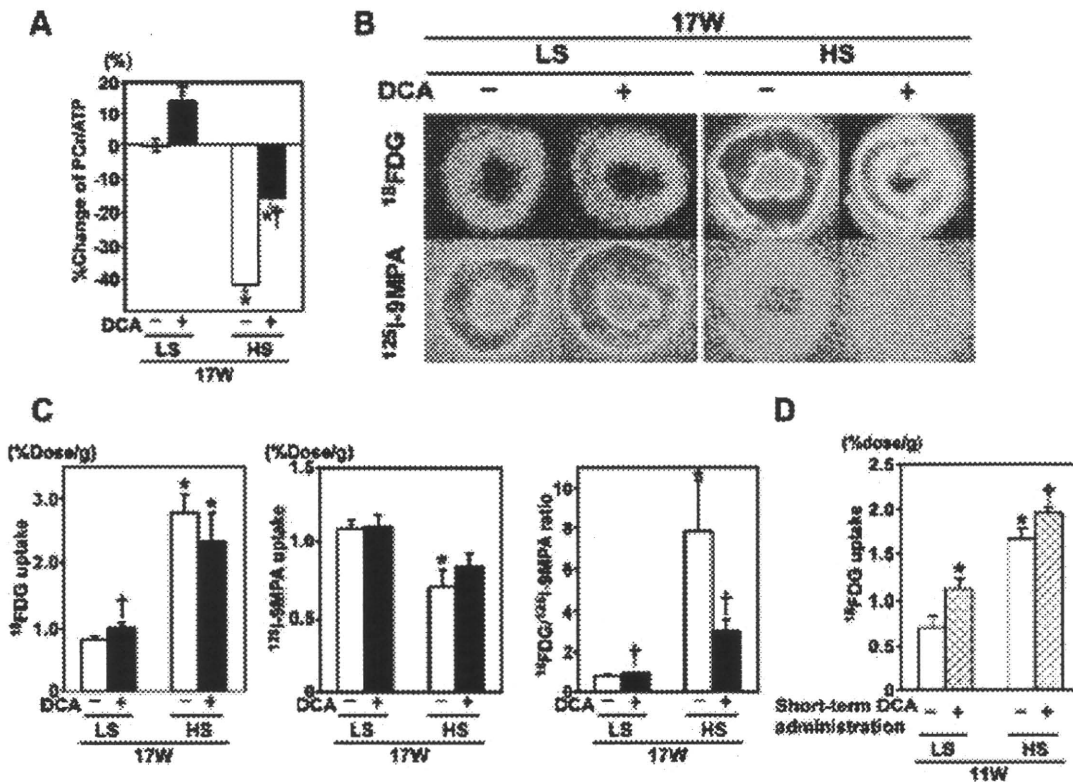


Figure 4. Effects of DCA on myocardial energy reserve and substrate utilization. A, Chronic DCA administration increased cardiac PCr/ATP in both control and CHF rats. B and C, DCA increased ^{18}F FDG uptake in normal rats but did not change ^{125}I -9MPA uptake. DCA tended to decrease ^{18}F FDG uptake and increase ^{125}I -9MPA uptake in CHF rats. The increase of ^{18}F FDG/ ^{125}I -9MPA in CHF rats was significantly reduced by DCA. * $P < 0.05$ vs control rats with vehicle or DCA. † $P < 0.05$ vs vehicle-treated rats on the same diet. $n = 6-10$ for LS diet and $n = 16-19$ for HS diet. D, Short-term DCA administration increased ^{18}F FDG uptake in control and LVH rats. * $P < 0.05$ vs control rats. † $P = 0.07$ vs vehicle-treated LVH rats; $n = 6-8$.

of CHF rats was increased (Figure 3F and supplemental Table VI). DCA lowered plasma lactate and pyruvate levels in HS+DCA rats, suggesting that DCA activated PDH and facilitated the entry of pyruvate and lactate into cells.

Effects of DCA on Myocardial Energy Reserve and Substrate Uptake

The administration of DCA increased PCr/ATP in rats that were fed an LS or HS diet (Figure 4A). Long-term DCA administration increased ^{18}F FDG uptake in normal rats but did not change ^{125}I -9MPA uptake (Figure 4B and 4C). DCA tended to decrease ^{18}F FDG uptake and increase ^{125}I -9MPA uptake in CHF rats. The increased ^{18}F FDG/ ^{125}I -9MPA of CHF rats was significantly reduced by DCA.

The attenuation of ^{18}F FDG uptake by DCA in CHF rats may be a secondary event due to the improvement of CHF by long-term DCA administration. To examine the direct effect of DCA, we examined the effect of short-term DCA administration on ^{18}F FDG uptake at 11 weeks of age, when DCA administration was started in the long-term experiment. Short-term DCA administration increased the uptake of ^{18}F FDG in both control and hypertrophied hearts (Figure 4D). In addition, long-term administration of DCA to control rats increased ^{18}F FDG uptake, PDH activity, and the PCr/ATP, suggesting DCA enhanced glucose oxidation and cardiac energy production. Thus, it is likely that DCA primarily

increased glucose oxidation and energy production and ameliorated CHF. DCA attenuated the changes in expression of several genes in CHF hearts (Figure 5 and supplemental Table IV). DCA augmented the decrease of peroxisome proliferator-activated receptor- α and nuclear receptor factor 1 gene expressions.

Metabolomic Profile of the Transition From Hypertrophy to Heart Failure

We measured the amounts of metabolites from glycolysis and the TCA cycle, as well as nucleotides and amino acids, by capillary electrophoresis time-of-flight mass spectrometry.²³⁻²⁵ The results of the quantification of all metabolites examined are listed in supplemental Table VII.

The result of the metabolome analysis of glycolysis and the TCA cycle is shown in Figure 6A. Pyruvate increased, alanine decreased, and succinate decreased in the heart tissues of CHF rats. However, it was difficult to estimate the flux of glycolysis or the TCA cycle based on a "snapshot" quantification of the metabolites. The energy metabolism of a cell is regulated at multiple levels, such as gene and protein expression and multiple posttranslational modifications of protein. Because preservation of energy production is essential to the survival of cells, impairment of the system is compensated for by multiple mechanisms, and the change in the amount of metabolites is smaller than the changes of gene or protein expression of enzymes.²⁴

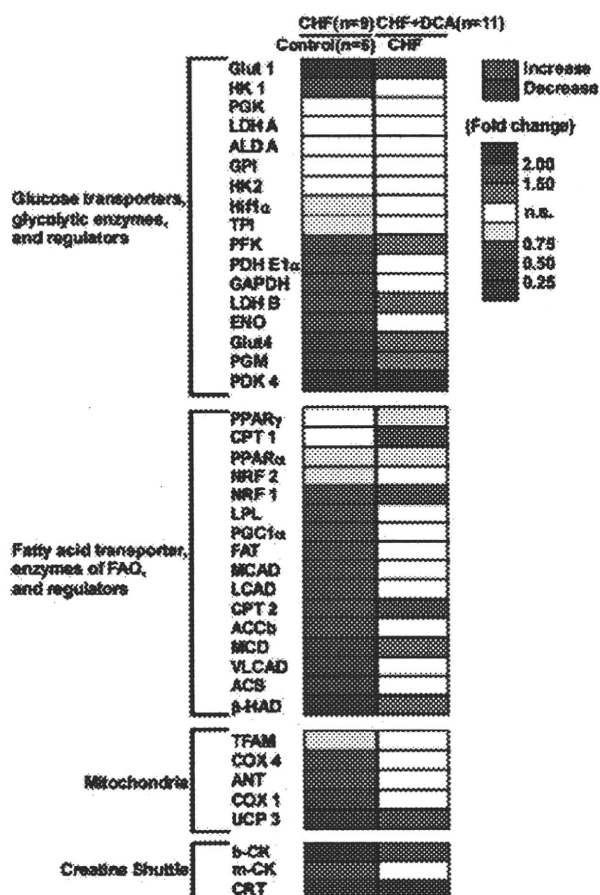


Figure 5. Effects of DCA on myocardial gene expression. The gene expression related to energy metabolism was compared between control and CHF rats (left column). Red indicates increase and blue indicates decrease compared with control rats. The gene expression was also compared between CHF and CHF+DCA (right column). Red indicates increase and blue indicates decrease compared with CHF rats.

A pathway in which we could estimate flux was the pentose phosphate pathway (PPP) (Figure 6B). The PPP derives from a glycolytic pathway via glucose 6-phosphate, which is also an intermediate of glycolysis. The pathway recycles the reduced form of nicotinamide adenine dinucleotide phosphate (NADPH), which makes reduced glutathione (GSH) to neutralize oxidative stress, thus regulating the cellular redox state. The NADPH/NADP⁺ (oxidized form) increased at the CHF stage and was further increased by DCA. DCA also increased levels of both GSH and oxidized glutathione (GSSG). Moreover, ophthalmate is reported to be a sensitive indicator of oxidative stress and is thought to be synthesized through the same by enzymes of glutathione synthesis.²⁵ Feedback inhibition of ophthalmate synthesis by GSH resulted in a reduced level of ophthalmate in the reducing state. Our results showed an increase in GSH with a concurrent decrease in ophthalmate on DCA treatment.

Confirmation of the Metabolome Analysis

To confirm the results of the metabolome analysis, amounts of metabolites of PPP were measured by enzyme recycling methods (supplemental Figure IVA and IVB). The NADPH/

NADP⁺ was increased in CHF rats and was increased by DCA in both control and CHF rats. The GSH/GSSG was significantly increased by DCA treatment in CHF rats.

PPP Was Activated at the CHF Stage or by DCA in Rat Hearts

To examine whether the increase in NADPH/NADP⁺ was due to activation of PPP, we examined the gene expression, protein expression, and enzymatic activity of glucose 6-phosphate dehydrogenase (G6PD), a rate-limiting enzyme of PPP in heart tissue. G6PD activity was increased at the CHF stage or by DCA (Figure 7A). Inhibition of G6PD by dehydroepiandrosterone (DHEA) sulfate attenuated the DCA-induced increase in NADPH/NADP⁺, suggesting DCA increased the ratio by activating PPP (Figure 7B).

DCA Reduced Oxidative Stress in DS Rat Hearts

Because the increase in NADPH and GSH reduces oxidative stress and oxidative stress is implicated in CHF,²⁶ we examined the effect of DCA on markers of oxidative stress. Thiobarbituric acid-reactive substances (TBARS), a marker of lipid peroxidation, increased at the CHF stage, and DCA attenuated the increase (Figure 7C). The amount of 4-hydroxy-2-nonenal-modified proteins, an index of protein peroxidation, increased at the CHF stage, and DCA attenuated the increase (Figure 7D).

DCA Attenuated Myocyte Cell Death in a PPP-Dependent Manner

Next, we investigated the effect of DCA on the survival of cultured myocytes. DCA protected myocytes in a dose-dependent manner from H₂O₂-induced cell death (Figure 8A). Pharmacologic inhibition of G6PD with DHEA or 6-aminonicotinamide indicated the protective effect of DCA to be dependent on PPP (Figure 8B). Small interfering RNAs of G6PD also abolished the protective effect of DCA (supplemental Figure VA and VB). DCA increased G6PD activity, NADPH/NADP⁺, and GSH/GSSG, and the increases were attenuated by inhibitors (Figure 8C through 8E) and small interfering RNAs (supplemental Figure VC and VD) of G6PD. Furthermore, H₂O₂ increased the TBARS of cultured myocytes, and DCA attenuated the increase in a PPP-dependent manner (Figure 8F and supplemental Figure VE). Thus, DCA attenuated H₂O₂-induced myocyte cell death dependent on PPP.

Discussion

In this study, we characterized metabolic remodeling in compensated LVH and CHF. LVH or CHF was associated with a distinct change in the metabolic profile of the heart. DCA increased glucose uptake and cardiac energy reserves and ameliorated CHF. Thus, alteration of cardiac energy metabolism is not an epiphenomenon but a cause of CHF, and long-term administration of DCA may be a useful therapeutic modality for CHF. The metabolome analysis indicated activation of PPP in CHF. PPP was also activated by DCA, and DCA protected myocytes from oxidative stress-induced cell death, suggesting activation of PPP by increased glucose metabolism to be a protective mechanism in CHF.

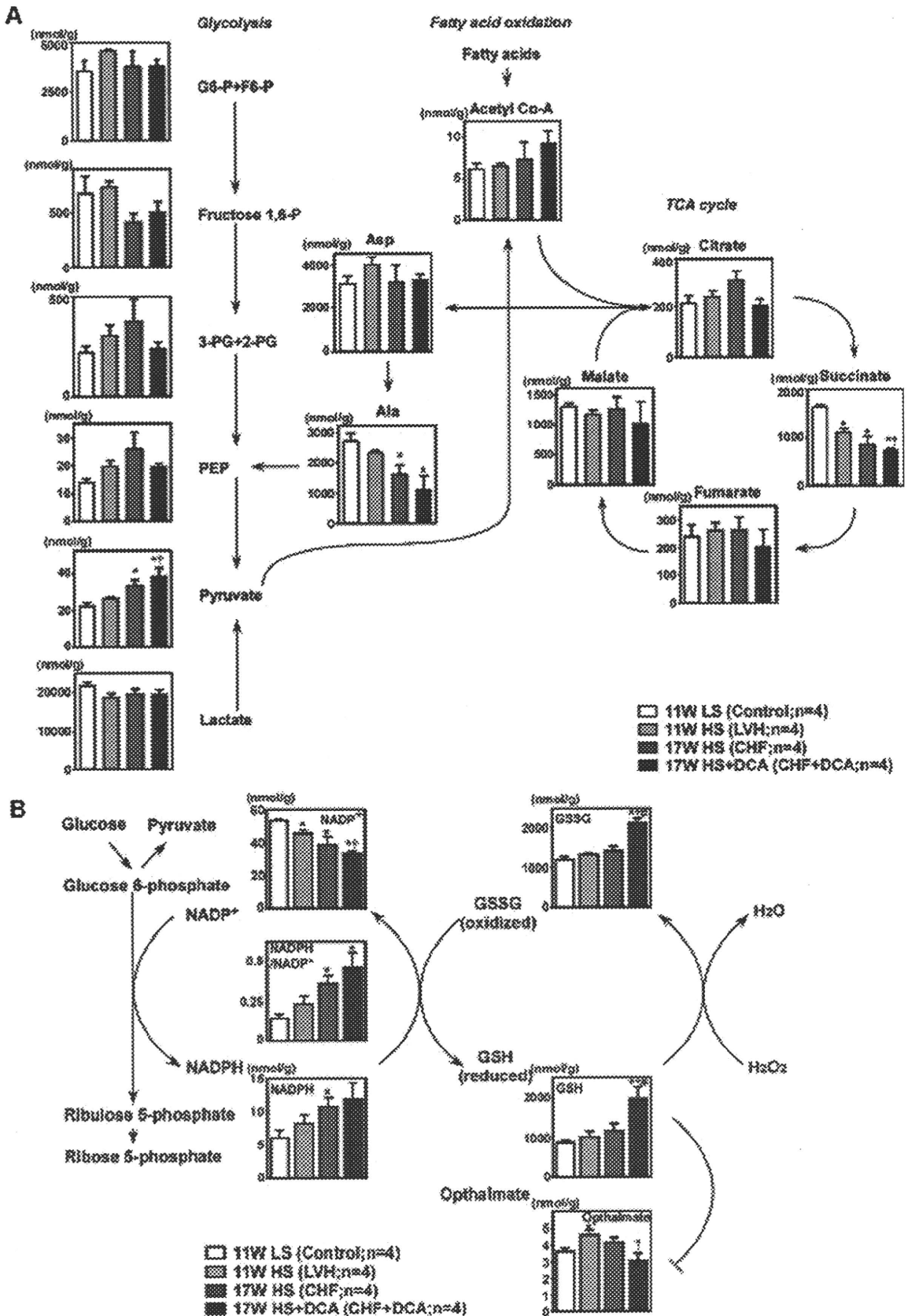


Figure 6. Metabolic profile of the transition from LVH to CHF. **A**, Metabolites of glycolysis and the TCA cycle. **B**, Metabolites of PPP. **P*<0.05 vs control rats. †*P*<0.05 vs LVH rats. #*P*<0.05 vs CHF rats.

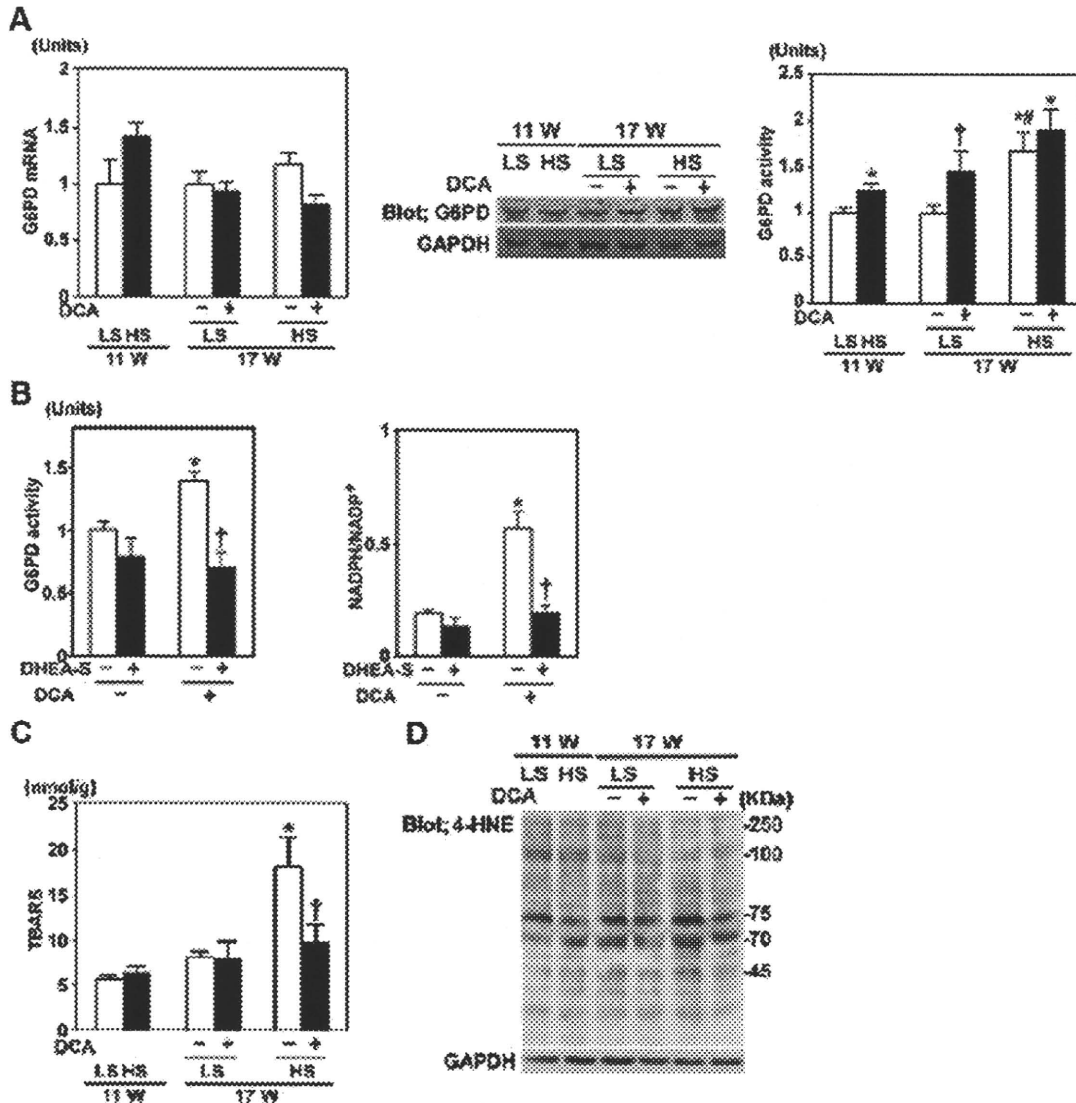


Figure 7. G6PD was activated at the CHF stage or by DCA. A, Gene and protein expressions of G6PD did not differ between the groups. The G6PD activity was increased at the CHF stage or by DCA. The mean value for control rats was defined as 1 unit; n=6–8 for each group. *P<0.05 vs control rats with vehicle or DCA. †P<0.05 vs vehicle-treated rats on the same diet. #P<0.05 vs LVH rats. B, DHEA sulfate decreased G6PD activity and NADPH/NADP⁺ in rats administered DCA; n=5. *P<0.05 vs rats without DCA. †P<0.05 vs rats without DHEA sulfate. C, Myocardial TBARS did not change at the LVH stage but increased at the CHF stage. DCA decreased TBARS of CHF rats; n=6–8. *P<0.05 vs control rats with vehicle or DCA. †P<0.05 vs vehicle-treated rats on the same diet. D, 4-Hydroxy-2-nonenal-modified protein was increased in CHF rats, and the increase was attenuated by DCA. A representative blot is shown, and GAPDH was used as a loading control.

NADPH increases were associated with increased G6PD activity at the CHF stage, suggesting that the flux of PPP was increased. DCA also increased G6PD activity and increased NADPH and GSH levels in a G6PD-dependent manner in rat hearts. G6PD protected cardiac myocytes from H₂O₂-induced cell death dependent on PPP. In addition, mice with reduced levels of G6PD activity developed cardiac dysfunction through increased susceptibility to reactive oxygen species.²⁷ Thus, activation of G6PD at the CHF stage is likely to be an adaptive mechanism. The mechanism by which CHF increases G6PD activity is unclear. Oxidative stress increased G6PD activity in the heart.²⁷ In addition, induction of mitochondrial dysfunction is associated with increased flux of glycolysis and PPP,²⁸ in which the amounts of pyruvate

and metabolites of PPP derived from isotope-labeled glucose increased. Indeed, the expression of genes and transcriptional regulators of mitochondrial function was decreased in our study, and reduced mitochondrial function in failing hearts has been reported.²⁶ In our study, pyruvate was increased in CHF rat hearts. Enhanced glycolysis may produce more pyruvate than is used in diseased mitochondria and thus cause pyruvate to accumulate. The mechanism by which DCA increased G6PD activity and PPP also needs to be clarified. The increase of GSH by DCA in cardiomyocytes has been reported.²⁹

One purpose of this study was to obtain a comprehensive metabolic profile of compensated LVH and decompensated heart failure in an in situ condition, because energy metabolism of a cell is highly dependent on the environment²⁴ and

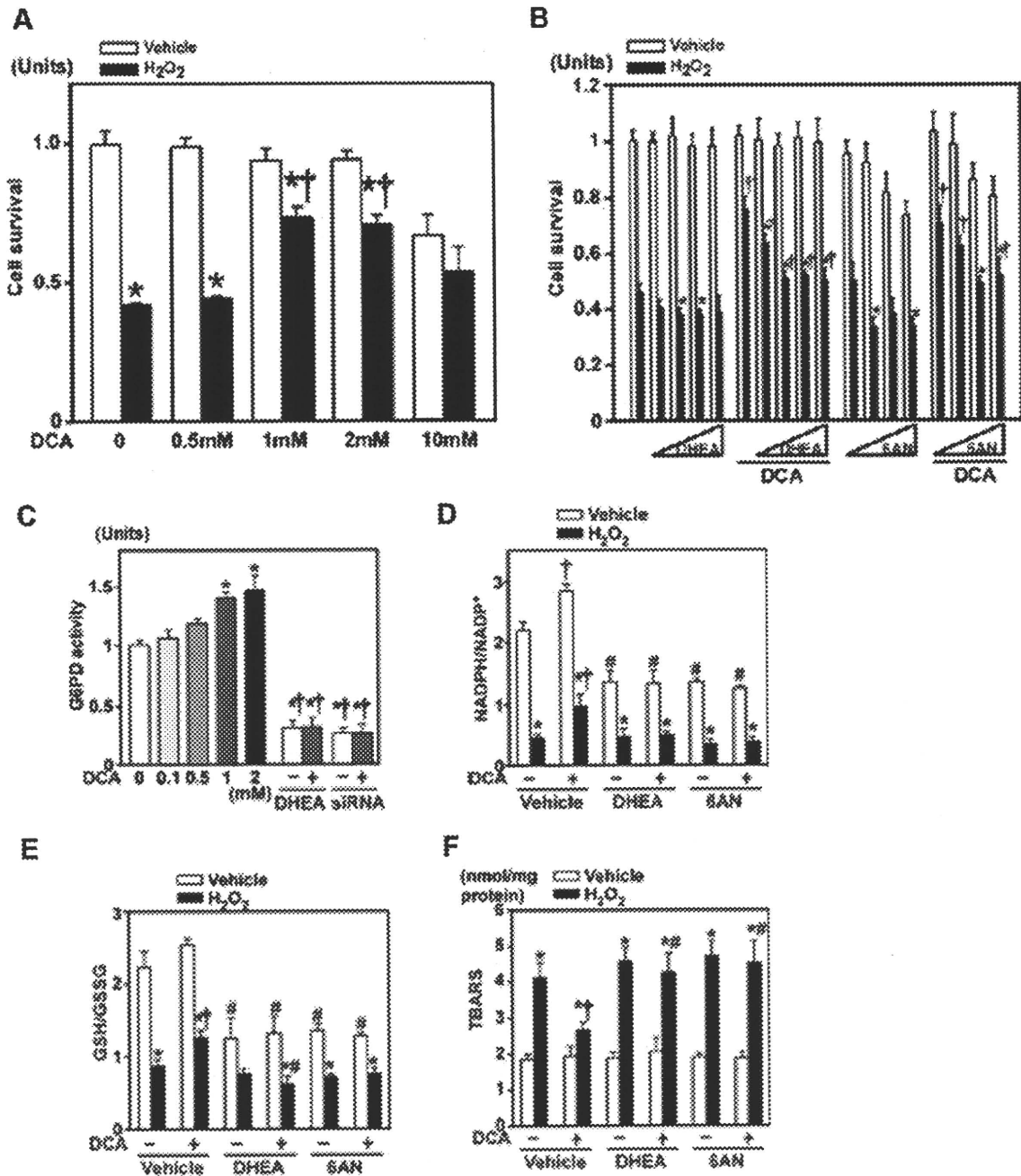


Figure 8. DCA attenuated myocyte cell death in a PPP-dependent manner. A, DCA attenuated H₂O₂-induced cardiomyocyte death in a dose-dependent manner up to 2 mmol/L. The mean value of the group without treatment was expressed as 1 unit. **P*<0.05 vs cardiomyocytes without H₂O₂. †*P*<0.05 vs H₂O₂-treated cardiomyocytes without DCA. B, Inhibition of PPP suppressed the protective effect of DCA in cultured myocytes. Three, 10, 30, or 100 μmol/L of DHEA was used; 10, 100, or 300 μmol/L or 1 mmol/L of 6-aminonicotinamide (6AN) was used. **P*<0.05 vs H₂O₂-treated cardiomyocytes without an inhibitor. †*P*<0.05 vs H₂O₂-treated cardiomyocytes without DCA. C, DCA increased G6PD activity, and the increase was suppressed by an inhibitor or siRNA. **P*<0.05 vs cardiomyocytes without DCA. †*P*<0.05 vs cardiomyocytes without G6PD inhibition. D and E, DCA increased NADPH/NADP⁺ and GSH/GSSG, and these changes were suppressed by inhibiting G6PD. F, TBARS were increased by H₂O₂, and the increase was attenuated by DCA in cultured myocytes. The effect of DCA was suppressed by G6PD inhibitors. **P*<0.05 vs cardiomyocytes without H₂O₂. †*P*<0.05 vs cardiomyocytes without DCA. #*P*<0.05 vs cardiomyocytes without inhibitor; n=9–18 samples for each group.

the results obtained from experiments in ex vivo perfused hearts are highly dependent on the substrate in the perfusion buffer, work load, and differences in cardiac function between control and failing hearts.³⁰ Glucose uptake was significantly increased at the CHF stage. However, it is unclear how this glucose was metabolized in this study.

Glucose is converted to pyruvate via glycolysis, and pyruvate is metabolized in the mitochondria by oxidation, namely, glucose oxidation. Glucose is also metabolized via other pathways, such as PPP. In humans or large animals, glucose metabolism in the heart can be measured in situ by infusing isotope-labeled glucose and collecting blood samples from

the coronary sinus or by using multiple cardiac substrates labeled with positron-emitting isotopes. Although it is difficult to measure glucose metabolism in situ in the hearts of small animals, we speculate that glycolysis was increased in CHF rat hearts in the presence of decreased gene expression of glycolytic enzymes for the following reasons. First, the gene expression of glycolytic enzymes is paradoxically downregulated in the presence of enhanced glucose oxidation in a canine model of heart failure.³¹ Second, the gene expression of glycolytic enzymes is decreased in failing human hearts,³² and glucose metabolism is increased in failing human hearts.³³ Third, using *ex vivo* perfused heart preparations, several investigators found glycolysis to be increased in hypertrophied hearts of small animals.^{34,35} However, whether increased glycolysis is coupled to glucose oxidation is controversial,³⁵ and the increase in pyruvate at the CHF stage may indicate that glycolysis increased, independent of glucose oxidation. In addition, it is also likely that increased glucose uptake reflects increased glucose metabolism other than glucose oxidation, such as PPP. The fate of glucose needs to be determined in future studies by injecting isotope-labeled glucose and measuring metabolites.^{36,37}

We performed a metabolome analysis by capillary electrophoresis time-of-flight mass spectrometry. Unfortunately, we could not determine the amounts of metabolites in fatty acid metabolism because they are electronically uncharged and cannot be separated by electrophoresis. However, we speculate that FAO was decreased at the CHF stage because the expression of genes and proteins related to FAO and mitochondrial function was decreased, fatty acid uptake decreased, and the PCr/ATP was significantly decreased. In addition, decreased FAO has been consistently reported in animal models of CHF and in patients with CHF.^{2,30,33}

Recently, Pound et al³⁸ reported that DCA increased glucose oxidation and improved cardiac contractility of *ex vivo* perfused hypertrophied hearts. In that study, they showed that carboxylation of pyruvate via a cytosolic malic enzyme instead of PDH produced a malate and enabled the anaplerotic influx of carbon into the TCA cycle. The anaplerotic flux through malic enzyme consumes NADPH. Pound et al reported that malate increased in hypertrophied hearts, but malate levels did not change at the LVH or CHF stage in our study. The difference may be due to the experimental conditions used. NADPH increased, rather than decreased, in our study, suggesting PPP to be a major source of NADPH in cells.³⁹

Because the oxygen consumption of LVH hearts in this rat model is significantly increased,⁴⁰ the mild decrease of energy reserves in situ may be due to an increase in energy consumption rather than a decrease in energy production. LVH was associated with unchanged fatty acid uptake, increased glucose uptake, and preserved gene and protein expression related to FAO and mitochondrial function, suggesting that an alteration of energy metabolism at the LVH stage largely depended on posttranscriptional mechanisms. At the CHF stage, oxygen consumption was decreased⁴⁰ and cardiac energy reserve was markedly decreased, suggesting that energy production was likely to be decreased. CHF is associated with decreased fatty acid uptake, a further increase in glucose uptake, and increased reactive oxygen species

production. Because a global change in gene expression related to energy production was a characteristic of the CHF stage, transcriptional regulation may be important in metabolic remodeling during the transition from LVH to CHF. It may be hypothesized that decreased expression of genes related to mitochondrial function causes a significant reduction in energy reserves and enhances glycolysis via a posttranscriptional mechanism, such as the Randle reaction, to compensate for the decreased energy reserves. The increased glucose metabolism may also attenuate oxidative stress by activating PPP. Further studies are needed to test this hypothesis.

Sources of Funding

This study received grants from the Japan Society for the Promotion of Science, the Japan Heart Foundation, the Japan Foundation of Cardiovascular Research, NOVARTIS Foundation for the Promotion of Science, the Mochida Memorial Foundation for Medical and Pharmaceutical Research, the Takeda Medical Research Foundation, the Kanagawa Nanryo Foundation, the Takeda Science Foundation, the Vehicle Racing Commemorative Foundation, and the Innovative Techno-Hub for Integrated Medical Bio-imaging Project of the Special Coordination Funds for Promoting Science and Technology.

Disclosures

None.

References

- Herrmann G, Decherd GM. The chemical nature of heart failure. *Ann Intern Med.* 1939;12:1233–1244.
- Neubauer S. The failing heart—an engine out of fuel. *N Engl J Med.* 2007;356:1140–1151.
- Stanley WC, Recchia FA, Lopaschuk GD. Myocardial substrate metabolism in the normal and failing heart. *Physiol Rev.* 2005;85:1093–1129.
- Casademont J, Miro O. Electron transport chain defects in heart failure. *Heart Fail Rev.* 2002;7:131–139.
- Weiss RG, Gerstenblith G, Bottomley PA. ATP flux through creatine kinase in the normal, stressed, and failing human heart. *Proc Natl Acad Sci U S A.* 2005;102:808–813.
- Stacpoole PW, Kurtz TL, Han Z, Langaee T. Role of dichloroacetate in the treatment of genetic mitochondrial diseases. *Adv Drug Deliv Reviews.* 2008;60:1478–1487.
- Stacpoole PW, Wright EC, Baumgartner TG, Bersin RM, Buchalter S, Curry SH, Duncan CA, Harman EM, Henderson GN, Jenkinson S. A controlled clinical trial of dichloroacetate for treatment of lactic acidosis in adults. The Dichloroacetate-Lactic Acidosis Study Group. *N Engl J Med.* 1992;327:1564–1569.
- Michelakis ED, McMurry MS, Wu XC, Dyck JR, Moudgil R, Hopkins TA, Lopaschuk GD, Puttagunta L, Waite R, Archer SL. Dichloroacetate, a metabolic modulator, prevents and reverses chronic hypoxic pulmonary hypertension in rats: role of increased expression and activity of voltage-gated potassium channels. *Circulation.* 2002;105:244–250.
- Bonnet S, Archer SL, Allalunis-Turner J, Haromy A, Beaulieu C, Thompson R, Lee CT, Lopaschuk GD, Puttagunta L, Bonnet S, Harry G, Hashimoto K, Porter CJ, Andrade MA, Thebaud B, Michelakis ED. A mitochondria-K⁺ channel axis is suppressed in cancer and its normalization promotes apoptosis and inhibits cancer growth. *Cancer Cell.* 2007;11:37–51.
- Taniguchi M, Wilson C, Hunter CA, Pehowich DJ, Clanachan AS, Lopaschuk GD. Dichloroacetate improves cardiac efficiency after ischemia independent of changes in mitochondrial proton leak. *Am J Physiol Heart Circ Physiol.* 2001;280:H1762–H1769.
- Bersin RM, Wolfe C, Kwassman M, Lau D, Klinski C, Tanaka K, Khorrami P, Henderson GN, de Marco T, Chatterjee K. Improved hemodynamic function and mechanical efficiency in congestive heart failure with sodium dichloroacetate. *J Am Coll Cardiol.* 1994;23:1617–1624.
- Lewis JF, DaCosta M, Wargowich T, Stacpoole PW. Effects of dichloroacetate in patients with congestive heart failure. *Clin Cardiol.* 1998;21:888–892.

13. Inoko M, Kihara Y, Morii I, Fujiwara H, Sasayama S. Transition from compensatory hypertrophy to dilated, failing left ventricles in Dahl salt-sensitive rats. *Am J Physiol*. 1994;267:H2471–H2482.
14. Fujii N, Nozawa T, Igawa A, Kato B, Igarashi N, Nonomura M, Asanoi H, Tazawa S, Inoue M, Inoue H. Saturated glucose uptake capacity and impaired fatty acid oxidation in hypertensive hearts before development of heart failure. *Am J Physiol Heart Circ Physiol*. 2004;287:H760–H766.
15. Dang CV, Semenza GL. Oncogenic alterations of metabolism. *Trends Biochem Sci*. 1999;24:68–72.
16. Sano M, Minamoto T, Toko H, Miyauchi H, Orimo M, Qin Y, Akazawa H, Tateno K, Kayama Y, Harada M, Shimizu I, Asahara T, Hamada H, Tomita S, Molkenin JD, Zou Y, Komuro I. p53-induced inhibition of Hif-1 causes cardiac dysfunction during pressure overload. *Nature*. 2007;446:444–448.
17. Sack MN, Rader TA, Park S, Bastin J, McCune SA, Kelly DP. Fatty acid oxidation enzyme gene expression is downregulated in the failing heart. *Circulation*. 1996;94:2837–2842.
18. Finck BN, Kelly DP. PGC-1 coactivators: inducible regulators of energy metabolism in health and disease. *J Clin Invest*. 2006;116:615–622.
19. Sano M, Schneider MD. Energizer: PGC-1 α keeps the heart going. *Cell Metab*. 2005;1:216–218.
20. Neubauer S, Frank M, Hu K, Remkes H, Laser A, Horn M, Ertl G, Lohse MJ. Changes of creatine kinase gene expression in rat heart post-myocardial infarction. *J Mol Cell Cardiol*. 1998;30:803–810.
21. Long YC, Zierath JR. AMP-activated protein kinase signaling in metabolic regulation. *J Clin Invest*. 2006;116:1776–1783.
22. Tian R, Musi N, D'Agostino J, Hirshman MF, Goodyear LJ. Increased adenosine monophosphate-activated protein kinase activity in rat hearts with pressure-overload hypertrophy. *Circulation*. 2001;104:1664–1669.
23. Soga T, Ohashi Y, Ueno Y, Naraoka H, Tomita M, Nishioka T. Quantitative metabolome analysis using capillary electrophoresis mass spectrometry. *J Proteome Res*. 2003;2:488–494.
24. Ishii N, Nakahigashi K, Baba T, Robert M, Soga T, Kanai A, Hirasawa T, Naba M, Hirai K, Hoque A, Ho PY, Kakazu Y, Sugawara K, Igarashi S, Harada S, Masuda T, Sugiyama N, Togashi T, Hasegawa M, Takai Y, Yugi K, Arakawa K, Iwata N, Toya Y, Nakayama Y, Nishioka T, Shimizu K, Mori H, Tomita M. Multiple high-throughput analyses monitor the response of *E. coli* to perturbations. *Science*. 2007;316:593–597.
25. Soga T, Baran R, Suematsu M, Ueno Y, Ikeda S, Sakurakawa T, Kakazu Y, Ishikawa T, Robert M, Nishioka T, Tomita M. Differential metabolomics reveals ophthalmic acid as an oxidative stress biomarker indicating hepatic glutathione consumption. *J Biol Chem*. 2006;281:16768–16776.
26. Ide T, Tsutsui H, Hayashidani S, Kang D, Suematsu N, Nakamura K, Utsumi H, Hamasaki N, Takeshita A. Mitochondrial DNA damage and dysfunction associated with oxidative stress in failing hearts after myocardial infarction. *Circ Res*. 2001;88:529–535.
27. Jain M, Cui L, Brenner DA, Wang B, Handy DE, Leopold JA, Loscalzo J, Apstein CS, Liao R. Increased myocardial dysfunction after ischemia-reperfusion in mice lacking glucose-6-phosphate dehydrogenase. *Circulation*. 2004;109:898–903.
28. Endo J, Sano M, Katayama T, Hishiki T, Shinmura K, Morizane S, Matsuhashi T, Katsumata Y, Zhang Y, Ito H, Nagahata Y, Marchitti S, Nishimaki K, Wolf AM, Nakanishi H, Hattori F, Vasilios V, Adachi T, Ohsawa I, Taguchi R, Hirabayashi Y, Ohta S, Suematsu M, Ogawa S, Fukuda K. Metabolic remodeling induced by mitochondrial aldehyde stress stimulates tolerance to oxidative stress in the heart. *Circ Res*. 2009;105:1118–1127.
29. Li S, Li X, Li YL, Shao CH, Bidasee KR, Rozanski GJ. Insulin regulation of glutathione and contractile phenotype in diabetic rat ventricular myocytes. *Am J Physiol Heart Circ Physiol*. 2007;292:H1619–H1629.
30. van Bilsen M, van Nieuwenhoven FA, van der Vusse GJ. Metabolic remodeling of the failing heart: beneficial or detrimental? *Cardiovasc Res*. 2009;81:420–428.
31. Lei B, Lionetti V, Young ME, Chandler MP, d'Agostino C, Kang E, Altarejos M, Matsuo K, Hintze TH, Stanley WC, Recchia FA. Paradoxical downregulation of the glucose oxidation pathway despite enhanced flux in severe heart failure. *J Mol Cell Cardiol*. 2004;36:567–576.
32. Razeghi P, Young ME, Alcorn JL, Moravec CS, Frazier OH, Taegtmeier H. Metabolic gene expression in fetal and failing human heart. *Circulation*. 2001;104:2923–2931.
33. Dávila-Román VG, Vedala G, Herrero P, de las Fuentes L, Rogers JG, Kelly DP, Gropler RJ. Altered myocardial fatty acid and glucose metabolism in idiopathic dilated cardiomyopathy. *J Am Coll Cardiol*. 2002;40:271–277.
34. Nascimben L, Ingwall JS, Lorell BH, Pinz I, Schultz V, Tornheim K, Tian R. Mechanisms for increased glycolysis in the hypertrophied rat heart. *Hypertension*. 2004;44:623–624.
35. Leong HS, Brownsey RW, Kulpa JE, Allard MF. Glycolysis and pyruvate oxidation in cardiac hypertrophy—why so unbalanced? *Comp Biochem Physiol A Mol Integr Physiol*. 2003;135:499–513.
36. Patel AB, de Graaf RA, Mason GF, Rothman DL, Shulman RG, Behar KL. The contribution of GABA to glutamate/glutamine cycling and energy metabolism in the rat cortex in vivo. *Proc Natl Acad Sci U S A*. 2005;102:5588–5593.
37. Metallo CM, Walther JL, Stephanopoulos G. Evaluation of ¹³C isotopic tracers for metabolic flux analysis in mammalian cells. *J Biotechnol*. 2009;144:167–174.
38. Pound KM, Sorokina N, Ballal K, Berkich DA, Fasano M, Lanoue KF, Taegtmeier H, O'Donnell JM, Lewandowski ED. Substrate-enzyme competition attenuates upregulated anaplerotic flux through malic enzyme in hypertrophied rat heart and restores triacylglyceride content: attenuating upregulated anaplerosis in hypertrophy. *Circ Res*. 2009;104:805–812.
39. Xu Y, Zhang Z, Hu J, Stillman IE, Leopold JA, Handy DE, Loscalzo J, Stanton RC. Glucose-6-phosphate dehydrogenase-deficient mice have increased renal oxidative stress and increased albuminuria. *FASEB J*. 2010;24:609–616.
40. Morii I, Kihara Y, Inoko M, Sasayama S. Myocardial contractile efficiency and oxygen cost of contractility are preserved during transition from compensated hypertrophy to failure in rats with salt-sensitive hypertension. *Hypertension*. 1998;31:949–960.

CLINICAL PERSPECTIVE

Congestive heart failure (CHF) is associated with a significant change in energy metabolism of the heart, and this alteration has been hypothesized to be important in the progression of CHF. Because treatment that improves the prognosis of patients with CHF, such as with β -adrenergic receptor blockers or angiotensin-converting enzyme inhibitors, is energy-sparing, it is hoped that modulation of cardiac energy metabolism may ameliorate CHF. We analyzed cardiac energy metabolism in Dahl salt-sensitive rats that were fed a high-salt diet, which showed a transition from compensated left ventricular hypertrophy to CHF. Left ventricular hypertrophy or CHF was associated with a distinct change in the metabolic profile of the heart. Glucose uptake increased and fatty acid uptake decreased in CHF. On comprehensive metabolome analysis that simultaneously measured the levels of multiple metabolites in heart tissue, the pentose phosphate pathway that regulates the cellular redox state was found to be activated in CHF. Dichloroacetate, a compound known to enhance glucose oxidation, increased glucose uptake and the energy reserve and improved cardiac function and survival. Dichloroacetate also activated the pentose phosphate pathway, decreased oxidative stress, and prevented cell death of cultured cardiomyocytes. Thus, increased glucose metabolism in CHF is likely to act as a protective mechanism by increasing the energy reserve and decreasing oxidative stress via pentose phosphate pathway activation. In summary, modulating the energy metabolism of the heart is likely to be a promising modality of CHF treatment.

Ca²⁺/Calmodulin-Dependent Kinase II δ Causes Heart Failure by Accumulation of p53 in Dilated Cardiomyopathy

Haruhiro Toko, MD, PhD; Hidehisa Takahashi, MD, PhD; Yosuke Kayama, MD; Toru Oka, MD, PhD; Tohru Minamino, MD, PhD; Sho Okada, MD, PhD; Sachio Morimoto, PhD; Dong-Yun Zhan, PhD; Fumio Terasaki, MD, PhD; Mark E. Anderson, MD, PhD; Masashi Inoue, MD, PhD; Atsushi Yao, MD, PhD; Ryoza Nagai, MD, PhD; Yasushi Kitaura, MD, PhD; Toshiyuki Sasaguri, MD, PhD; Issei Komuro, MD, PhD

Background—Dilated cardiomyopathy (DCM), characterized by dilatation and dysfunction of the left ventricle, is an important cause of heart failure. Many mutations in various genes, including cytoskeletal protein genes and contractile protein genes, have been identified in DCM patients, but the mechanisms of how such mutations lead to DCM remain unknown.

Methods and Results—We established the mouse model of DCM by expressing a mutated cardiac α -actin gene, which has been reported in patients with DCM, in the heart (mActin-Tg). mActin-Tg mice showed gradual dilatation and dysfunction of the left ventricle, resulting in death by heart failure. The number of apoptotic cardiomyocytes and protein levels of p53 were increased in the hearts of mActin-Tg mice. Overexpression of Bcl-2 or downregulation of p53 decreased the number of apoptotic cardiomyocytes and improved cardiac function. This mouse model showed a decrease in myofilament calcium sensitivity and activation of calcium/calmodulin-dependent kinase II δ (CaMKII δ). The inhibition of CaMKII δ prevented the increase in p53 and apoptotic cardiomyocytes and ameliorated cardiac function.

Conclusion—CaMKII δ plays a critical role in the development of heart failure in part by accumulation of p53 and induction of cardiomyocyte apoptosis in the DCM mouse model. (*Circulation*. 2010;122:891-899.)

Key Words: apoptosis ■ CaMKII ■ cardiomyopathy ■ heart failure ■ genes, p53

Heart failure is an important cause of morbidity and mortality in many industrial countries, and dilated cardiomyopathy (DCM) is one of its major causes.¹ Although treatments for heart failure have been progressed well in both pharmacological and nonpharmacological aspects, mortality of DCM patients remains high, and the only treatment for DCM patients with severe symptoms is heart transplantation. Because the number of hearts for transplantation is limited, the development of novel therapies for DCM has been awaited.

Clinical Perspective on p 899

DCM, characterized by dilatation and impaired contraction of the left ventricle, is a multifactorial disease that includes both hereditary and acquired forms. The acquired forms of

DCM are caused by various factors.² Twenty percent to 35% of patients have hereditary forms,¹ and advances in molecular genetic studies during the last decade have revealed many mutations of various genes in DCM patients.³⁻⁵

Several hypotheses have been reported on the mechanisms of how gene mutations lead to DCM phenotypes. Mutations in genes encoding cytoskeletal proteins such as desmin and muscle LIM protein might disturb the interaction between the sarcomere and Z disk, resulting in impaired force transmission from the sarcomere to the surrounding syncytium.^{4,6} On the other hand, mutations in genes encoding contractile proteins such as α -tropomyosin and cardiac troponin T have been reported to induce the decrease in myofilament calcium (Ca²⁺) sensitivity.⁷ An increase in apoptotic cardiomyocytes and/or destruction of membrane structure by calpain activa-

Received January 6, 2010; accepted July 2, 2010.

From the Department of Cardiovascular Science and Medicine, Chiba University Graduate School of Medicine, Chiba, Japan (H. Toko, H. Takahashi, Y.K., T.O., T.M., S.O., I.K.); Department of Cardiovascular Medicine, Osaka University Graduate School of Medicine, Suita, Japan (T.O., I.K.); Department of Clinical Pharmacology, Kyusyu University Graduate School of Medicine, Fukuoka, Japan (S.M., D.Z., T.S.); Department of Internal Medicine III, Osaka Medical College, Takatsuki, Japan (F.T., Y.K.); Department of Internal Medicine, and Molecular Physiology and Biophysics, Carver College of Medicine, University of Iowa, Iowa City (M.E.A.); and Department of Cardiovascular Medicine, University of Tokyo Graduate School of Medicine, Tokyo, Japan (M.I., A.Y., R.N.).

The online-only Data Supplement is available with this article at <http://circ.ahajournals.org/cgi/content/full/CIRCULATIONAHA.109.935296/DC1>.

Correspondence to Issei Komuro, MD, PhD, Department of Cardiovascular Medicine, Osaka University Graduate School of Medicine, 2-2 Yamadaoka, Suita 565-0871, Japan. E-mail komuro-tky@umin.ac.jp

© 2010 American Heart Association, Inc.

Circulation is available at <http://circ.ahajournals.org>

DOI: 10.1161/CIRCULATIONAHA.109.935296

tion have been reported to play a critical role in mutant gene-induced cardiac dysfunction.^{8–10} However, the precise mechanisms remain largely unknown as a result, at least in part, of a lack of good animal models of DCM.

Several animal models of DCM have been reported.^{11–13} The *mdx* mouse is a model of Duchenne muscular dystrophy, which has mutations in the dystrophin gene.¹¹ Unlike humans, *mdx* mice rarely show cardiac abnormality, which has limited the utility of *mdx* mice as a model to examine the pathogenesis of DCM. Although Golden Retriever-based muscular dystrophy dogs show DCM phenotypes,¹² the muscular dystrophy dogs are very difficult to maintain and handle. Although BIO 14.6 hamsters lacking δ -sarcoglycan are a good model of DCM,¹³ it is difficult to apply genetic approaches to the hamster. To elucidate the molecular mechanisms of how gene mutations cause DCM, appropriate animal models, particularly mouse models, are necessary. We established here a mouse model of DCM by expressing a mutated cardiac α -actin gene (mActin-Tg), which has been reported in patients with DCM, in the heart.⁵ mActin-Tg mice showed gradual dilatation and dysfunction of the left ventricle, resulting in death by heart failure. These phenotypes of mActin-Tg mice were quite similar to those of human DCM. In this study, we examined the underlying mechanisms of how this gene mutation leads to DCM using the new mouse model of DCM.

Methods

Detailed experimental methods are described in the online-only Data Supplement.

Mice

We generated transgenic mice (mActin-Tg) that expressed a mutated cardiac α -actin (R312H) with an HA tag in the heart. This mutation has been reported in patients with DCM.⁵ Generation of transgenic mice with cardiac-restricted overexpression of human Bcl-2, AC3-I, or nuclear factor of activated T cell (NFAT)-luciferase has been described previously.^{14–16} Heterozygous p53-deficient mice were purchased from The Jackson Laboratory (Bar Harbor, Me).¹⁷ Wild-type littermates served as controls for all studies. KN-93 ($10 \mu\text{mol} \cdot \text{kg}^{-1} \cdot \text{d}^{-1}$) was used to inhibit activation of Ca^{2+} /calmodulin-dependent kinase II (CaMKII). Echocardiography was performed on conscious mice.

Histology

For detection of apoptotic cardiomyocytes, we performed terminal deoxynucleotidyl transferase-mediated dUTP nick-end labeling (TUNEL) staining, along with immunostaining for dystrophin.

Western Blot Analysis

Whole-cell lysates were resolved by SDS-PAGE. Western blot analyses were performed with some antibodies. The intensities of Western blot bands were measured with NIH ImageJ software (National Institutes of Health, Bethesda, Md).

Luciferase Assay

Left ventricles were homogenized in luciferase assay buffer as described previously.¹⁵

Force Measurements

A small fiber was dissected from the skinned left ventricular papillary muscle, and isometric force was measured as described previously.⁷

RNA Extraction and Quantitative Real-Time Polymerase Chain Reaction Analysis

Quantitative real-time polymerase chain reaction was performed with the LightCycler with the Taqman Universal Probe Library and LightCycler Master. Relative levels of gene expressions were normalized to the mouse GAPDH expression with the $\Delta\Delta\text{Ct}$ method.¹⁸

Statistical Analysis

Data are shown as mean \pm SEM. Multiple-group comparison was performed by 1-way ANOVA followed by the Bonferroni procedure for comparison of means. The *F* test was used to assess equal variances before comparison between 2 groups. Then, comparisons between 2 groups were performed with the Student *t* test (when $P > 0.05$ in the *F* test) and the Welch *t* test (when $P < 0.05$ in the *F* test). Survival rates were analyzed with the log-rank test. Values of $P < 0.05$ were considered statistically significant.

Results

DCM Model Mouse

Because there are few useful DCM mouse models, we first generated transgenic mice that expressed a cardiac α -actin R312H mutant with an HA tag under the control of α -myosin heavy chain promoter (mActin-Tg). We obtained 3 independent founders of the transgenic mice (lines 301, 307, and 311). The protein levels of the cardiac α -actin R312H mutant were 1.6-fold in line 301, 3.3-fold in line 307, and 2.2-fold in line 311 compared with those of endogenous cardiac α -actin (Figure 1A in the online-only Data Supplement). To confirm the expression of the transgene in cardiomyocytes, we performed immunohistological analyses with antibodies against HA and actinin. The mutated cardiac α -actin protein was colocalized with actinin, suggesting that the cardiac α -actin R312H mutant is incorporated into myofilaments (Figure 1B in the online-only Data Supplement). Cardiac systolic function was decreased in mActin-Tg mice at 10 months of age, and the reduction was well correlated with protein levels of the cardiac α -actin R312H mutant (Figure 1C in the online-only Data Supplement). To further investigate whether cardiac expression of the cardiac α -actin R312H mutant led to heart failure, we examined another transgenic mouse that expressed cardiac α -actin A331P mutant with an HA tag in the heart. This mutant has been reported to cause hypertrophic cardiomyopathy in human.¹⁹ We obtained 2 independent founders of the transgenic mice that expressed almost the same levels of the cardiac α -actin A331P mutant protein. Although the protein levels of the mutant in the A331P mutant transgenic mice were almost same as those of the R312H mutant in line 307, which had the highest expression (Figure 2 in the online-only Data Supplement), echocardiography revealed that there were no significant differences in cardiac systolic function, wall thickness, and left ventricular dimension between cardiac α -actin A331P mutant transgenic mice and their wild-type littermates (Table 1 in the online-only Data Supplement). Although it is not known at present why the expression of cardiac α -actin A331P mutant did not induce hypertrophic cardiomyopathy, these results suggest that cardiac dysfunction of mActin-Tg mice is due to cardiac expression of the cardiac α -actin R312H mutant in the heart, not to high-level expression of the cardiac α -actin protein with the tag (lines 307 and 311).

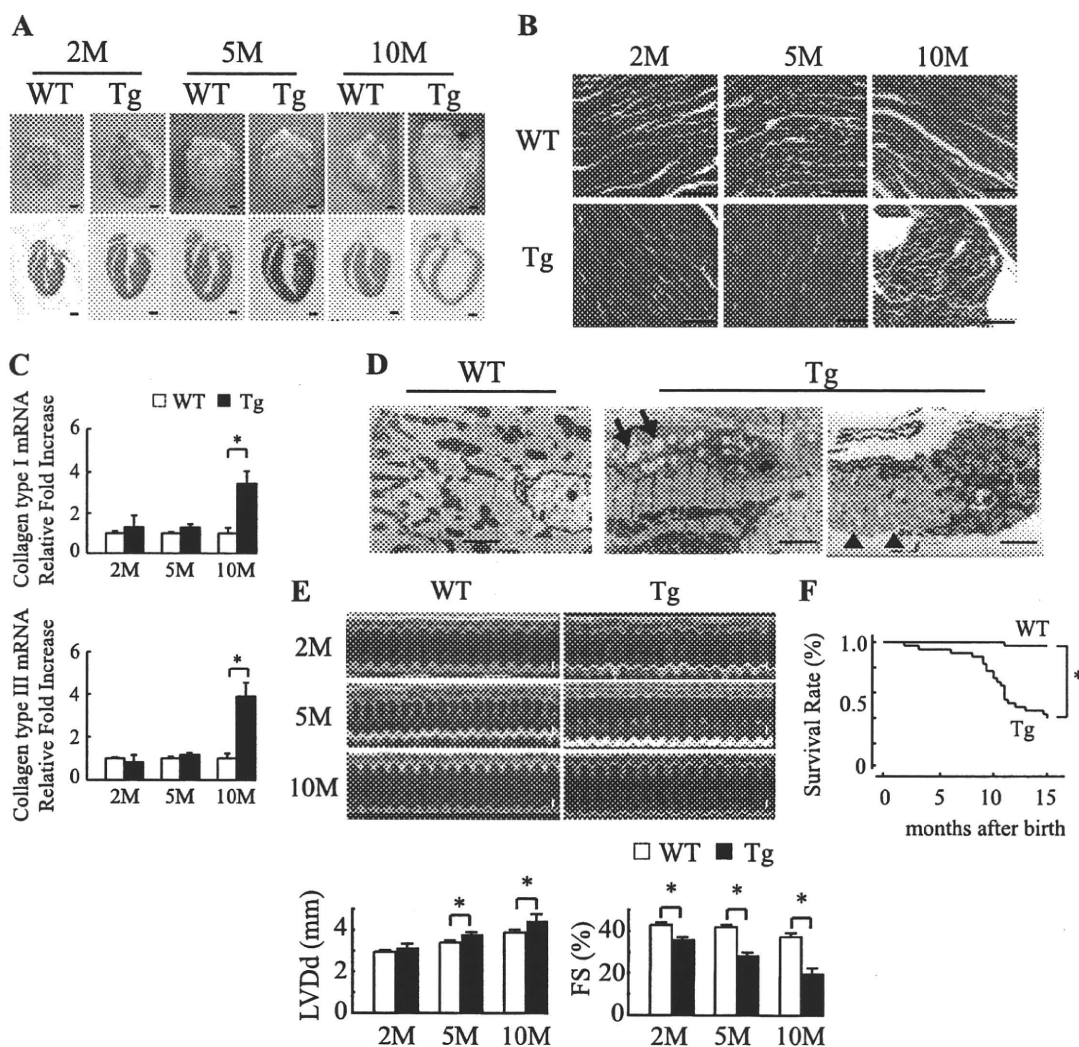


Figure 1. Mutated cardiac α -actin R312H transgenic mice. **A**, Gross morphology (top) and sections (bottom) of wild-type littermates (WT) or mActin-Tg (Tg) hearts at 2, 5, and 10 months (M) of age. Scale bar=1 mm. **B**, Masson trichrome staining. Scale bar=100 μ m. **C**, Relative levels of collagen types I and III in hearts were normalized to GAPDH expression. * P <0.05 vs WT mice. n =4 in each group. **D**, Electron microscopic analyses. Cytoplasmic vacuolization (arrow) and lysis of myofibrils (arrowhead) were detected in the hearts of Tg mice. Scale bar=10 μ m. **E**, Echocardiographic analysis. Scale bar=1 mm. LVDd indicates left ventricular end-diastolic dimension; FS, fractional shortening. * P <0.05. **F**, Kaplan-Meier survival curve. * P <0.05 vs WT mice. WT, n =32; Tg, n =37.

We used line 307, which expressed the cardiac α -actin R312H mutant at the highest levels, for further studies. The hearts in mActin-Tg mice were larger than those of wild-type littermates (Figure 1A), and heart weight and the ratio of heart weight to body weight were much increased in mActin-Tg mice (Table II in the online-only Data Supplement). Marked cardiac fibrosis was observed in mActin-Tg mice at 10 months of age, with increased expression of collagen types I and III (Figure 1B and 1C). Electron microscopic analyses showed that there were degenerated cardiomyocytes with an increase in vacuolar formation and lysis of myofibrils in mActin-Tg mice (Figure 1D). Echocardiography revealed that left ventricular dimension was gradually increased and that fractional shortening was reduced in mActin-Tg mice compared with wild-type littermates (Table II in the online-only Data Supplement and Figure 1E). The expression levels of ANP and SERCA2a were gradually

increased and decreased in mActin-Tg mice, respectively (Figure III in the online-only Data Supplement). There was no significant difference in blood pressure, but heart rate was increased in mActin-Tg mice (Table II in the online-only Data Supplement), suggesting that the sympathetic nervous system is activated. Surface ECG monitoring showed low amplitude of the R wave in mActin-Tg mice (Table II in the online-only Data Supplement), which is often observed in human DCM patients. Many mActin-Tg mice died by 35 weeks of age (Figure 1F). Although telemetric ECG recording did not show life-threatening arrhythmia in mActin-Tg mice (data not shown), spontaneous Ca^{2+} sparks and Ca^{2+} waves were significantly increased in the cardiomyocytes of mActin-Tg mice (Table III in the online-only Data Supplement), suggesting that not only cardiac pump failure but also arrhythmia could be the cause of death. These phenotypes of mActin-Tg mice were quite similar to those of human DCM.

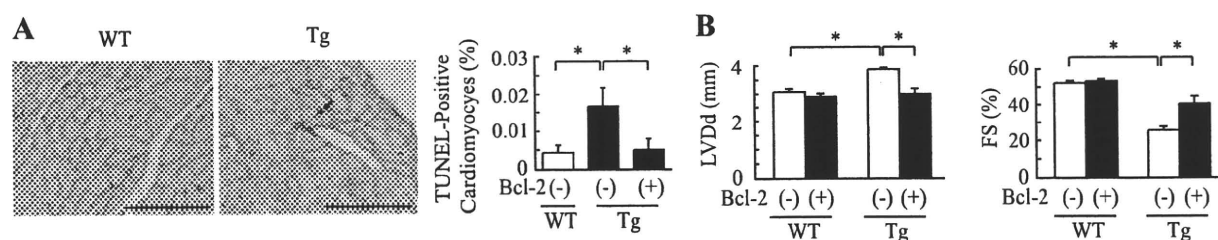


Figure 2. Increase in Bcl-2 preserves cardiac function in mActin-Tg mice. **A**, Double immunostaining for TUNEL (black) and dystrophin (red) of the heart (left). The graph indicates quantitative analyses of TUNEL-positive cardiomyocytes. Scale bar=100 μ m. $n=4$ in each group. $*P<0.05$. **B**, Echocardiographic analyses at 5 months of age. $*P<0.05$. WT/Bcl-2(-), $n=5$; WT/Bcl-2(+), $n=10$; Tg/Bcl-2(-), $n=10$; Tg/Bcl-2(+), $n=5$. WT indicates wild-type littermates; Tg, mActin-Tg mice; LVDD, left ventricular end-diastolic dimension; and FS, fractional shortening.

Apoptotic Cardiomyocytes Are Increased in mActin-Tg Hearts

It has been reported that apoptosis of cardiomyocytes is observed in hearts of human DCM¹⁰ and that cardiomyocyte death might cause cardiac dysfunction.²⁰ We thus examined apoptosis of cardiomyocytes by TUNEL labeling in left ventricular sections of wild-type littermates and mActin-Tg mice at 5 months of age. The number of TUNEL/dystrophin double-positive cardiomyocytes was significantly larger in mActin-Tg mice compared with wild-type littermates (Figure 2A). To examine whether the increase in apoptotic cardiomyocytes causes cardiac dysfunction in mActin-Tg mice, we generated double-transgenic mice by crossing mActin-Tg mice and the transgenic mice, which overexpress the antiapoptotic protein Bcl-2 in cardiomyocytes [mActin(+)/Bcl-2(+)-DTg].¹⁴ The number of apoptotic cardiomyocytes in mActin(+)/Bcl-2(+)-DTg mice was significantly less compared with mActin-Tg mice (Figure 2A). Echocardiography revealed that the left ventricular dimension was smaller and fractional shortening was better in mActin(+)/Bcl-2(+)-DTg mice than in mActin-Tg mice at 5 months of age (Figure 2B), suggesting that the increase in apoptotic cardiomyocytes causes cardiac dysfunction in the DCM mouse model.

p53 Is Involved in Cardiomyocyte Apoptosis in mActin-Tg Mice

To clarify the mechanisms of how the cardiac α -actin R312H mutant induces apoptosis of cardiomyocytes, we examined

expression levels of apoptosis-related proteins by Western blot analyses. The protein levels of p53 and Bax were higher in mActin-Tg mice compared with wild-type littermates (Figure 3A). Several key proapoptotic genes have been reported to be positively regulated by p53,²¹ and increased expression of p53 induces left ventricular dilatation and dysfunction in several types of mice.^{22,23} To determine the role of p53 in gene mutation-induced DCM, we crossed mActin-Tg mice and heterozygous p53-deficient mice [p53(+/-)]. Because many of homozygous p53-deficient mice [p53(-/-)] died of tumors before 5 months of age,¹⁷ we used heterozygous p53-deficient mice [p53(+/-)] for this study. Echocardiography revealed that left ventricular dimension was smaller and fractional shortening was better in mActin-Tg/p53(+/-) mice than in mActin-Tg/p53(+/+) mice at 5 months of age (Figure 3B). Loss of a single p53 allele attenuated the increase of Bax (Figure 3C) and reduced the number of apoptotic cardiomyocytes in mActin-Tg mice (Figure 3D). These results suggest that p53-induced cardiomyocyte apoptosis induces dilatation and dysfunction of the left ventricle in the DCM mouse model.

Myofilament Calcium Sensitivity Is Decreased and Calcium-Dependent Enzymes Are Activated in mActin-Tg Mice

Many gene mutations associated with DCM have been reported to induce the decrease of myofilament Ca^{2+} sensi-

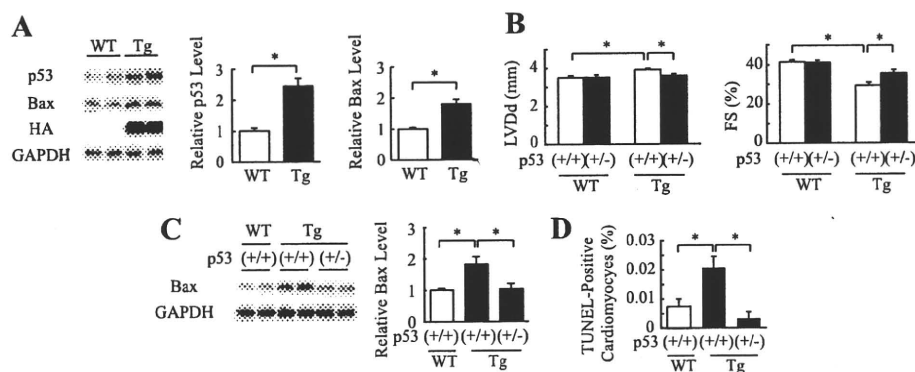


Figure 3. Inhibition of p53 preserves cardiac function in mActin-Tg mice. **A**, Western blot analyses in the hearts of wild-type littermates (WT) or mActin-Tg (Tg) mice at 5 months of age. The graph indicates relative protein levels of p53 ($n=8$ in each group) or Bax ($n=10$ in each group). $*P<0.05$. **B**, Echocardiographic analyses at 5 months of age. WT/p53(+/+), $n=12$; WT/p53(+/-), $n=10$; Tg/p53(+/+), $n=19$; Tg/p53(+/-), $n=14$. $*P<0.05$. **C**, Western blot analyses in the hearts. The graph indicates relative protein levels of Bax. $n=6$ in each group. $*P<0.05$. **D**, Quantitative analyses of TUNEL-positive cardiomyocytes. $n=5$ in each group. $*P<0.05$.

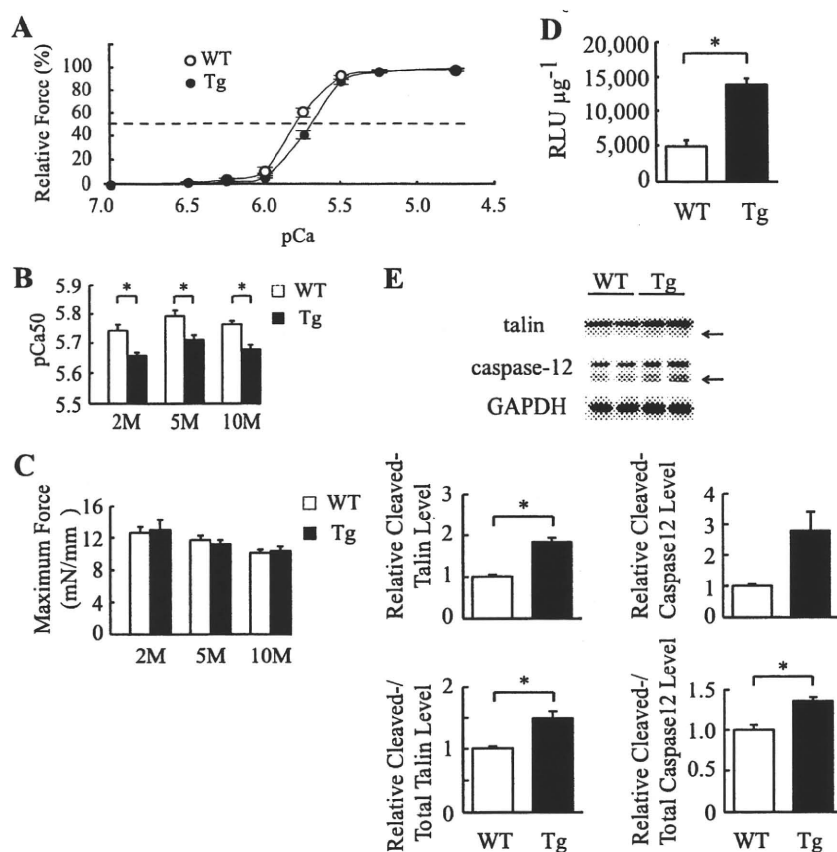


Figure 4. Myofilament Ca^{2+} sensitivity is decreased and Ca^{2+} -dependent enzymes are activated in mActin-Tg mice (Tg). **A**, Force-pCa relationship in skinned cardiac muscle fiber at 5 months of age. The broken line indicates pCa50. Wild-type (WT; $n=11$) and Tg ($n=10$) fibers were prepared from 3 isolated hearts. **B**, Ca^{2+} sensitivity (pCa50) of force-pCa relationships in skinned cardiac muscle fibers at 2, 5, and 10 months (M) of age. * $P<0.05$. **C**, Maximum force-generating capabilities. Fibers ($n=9$ to 11) were prepared from 3 isolated hearts of each group. **D**, The NFAT-luciferase reporter activity (RLU μg^{-1}) in the hearts at 5 months of age. $n=4$ in each group. * $P<0.05$. **E**, Western blot analyses in the hearts. Arrows indicate the calpain cleaved forms of talin and caspase-12. The graph indicates relative protein levels of cleaved talin or caspase-12 and ratio of cleaved forms to total proteins. $n=4$ in each group. * $P<0.05$.

tivity.⁷ We examined myofilament Ca^{2+} sensitivity in mActin-Tg mice. The force-pCa relationship was shifted rightward in mActin-Tg mice compared with wild-type littermates (Figure 4A). The pCa value at half-maximal force generation (pCa50, an index of Ca^{2+} sensitivity) was significantly lower in mActin-Tg mice (Figure 4B), suggesting that skinned cardiac muscle fibers prepared from mActin-Tg mice show a decrease in Ca^{2+} sensitivity of force generation. The degree was the same between 2 and 10 months of age (Figure 4B), suggesting that the reduction in Ca^{2+} sensitivity is not a result of cardiac dysfunction. Despite the reduced Ca^{2+} sensitivity, there was no significant difference in maximum force-generating capabilities between wild-type littermates and mActin-Tg mice (Figure 4C). The decrease in myofilament Ca^{2+} sensitivity is expected to influence intracellular Ca^{2+} handling in cardiomyocytes of mActin-Tg mice. To clarify whether intracellular Ca^{2+} levels in cardiomyocytes are changed in mActin-Tg mice, we examined the activity of Ca^{2+} -dependent enzymes such as calcineurin and calpain. We generated double-transgenic mice by crossing mActin-Tg mice and the transgenic mice carrying a luciferase reporter driven by a cluster of NFAT binding sites, which is activated by calcineurin-dependent NFAT proteins.¹⁵ The NFAT-luciferase reporter activity was higher in mActin-Tg mice than in wild-type littermates at 5 months of age (Table IV in the online-only Data Supplement and Figure 4D). Furthermore, the ratio of the calpain-induced cleaved forms of talin and caspase-12 to total proteins was significantly increased in mActin-Tg mice compared with wild-type littermates (Figure

4E). We next examined Ca^{2+} transients in cardiomyocytes using fluo-3AM (Figure IVA in the online-only Data Supplement). Although the time to peak amplitude of Ca^{2+} was significantly slower in mActin-Tg mice than in wild-type littermates (Figure IVB in the online-only Data Supplement), there was no significant difference in peak amplitude between wild-type littermates and mActin-Tg mice at 2 and 10 months of age (Figure IVC in the online-only Data Supplement). The expression levels of SERCA2a, but not $\text{Na}^+/\text{Ca}^{2+}$ exchanger, were decreased in mActin-Tg mice (Figure III in the online-only Data Supplement).

CaMKII δ Is Activated in mActin-Tg Mice

It has been reported that among Ca^{2+} -dependent proteins, expression of CaMKII δ is increased in human DCM hearts²⁴ and that overexpression of CaMKII δ induces heart failure in mice.^{25,26} We thus examined the expression and phosphorylation of CaMKII δ and phosphorylation of its target protein, phospholamban (Thr17). The protein levels of total (both CaMKII δB and CaMKII δC) and phosphorylated CaMKII δ and of phosphorylated phospholamban (Thr17) were increased in mActin-Tg mice compared with wild-type littermates (Figure 5A and Figure VA in the online-only Data Supplement), suggesting that CaMKII δ is activated in mActin-Tg mice. The protein levels of phosphorylated phospholamban (Ser16), which is activated by protein kinase A, were also increased in mActin-Tg mice (Figure 5A).

Because it has been reported that the sympathetic nervous system is activated in failing hearts and that β -adrenergic

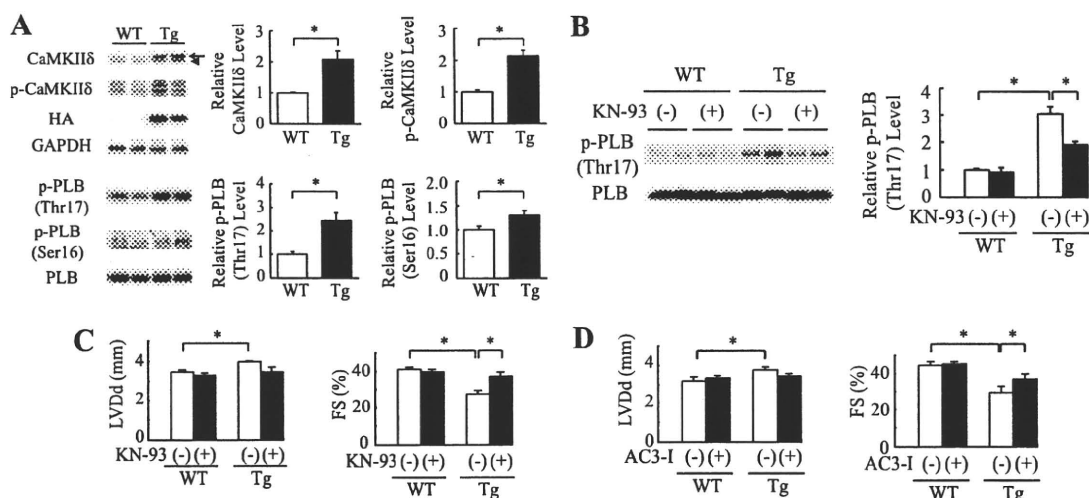


Figure 5. CaMKII δ is activated in mActin-Tg mice. **A**, Western blot analyses in the hearts of wild-type littermates (WT) or mActin-Tg (Tg) mice at 5 months of age. The graph indicates relative protein levels of total and phosphorylated CaMKII δ (p-CaMKII δ) or phosphorylated phospholamban (p-PLB). Arrow and arrowhead indicate CaMKII δ B and CaMKII δ C, respectively. $n=6$ in each group. $*P<0.05$. **B**, Western blot analyses in the hearts at 5 months of age. The graph indicates relative protein levels of p-PLB (Thr17). $n=4$ in each group. $*P<0.05$. **C** and **D**, Echocardiographic analyses at 5 months of age. WT/KN-93(-), $n=11$; WT/KN-93(+), $n=7$; Tg/KN-93(-), $n=8$; Tg/KN-93(+), $n=6$; WT/AC3-I(-), $n=8$; WT/AC3-I(+), $n=18$; Tg/AC3-I(-), $n=10$; Tg/AC3-I(+), $n=14$. KN indicates KN-93; LVDD, left ventricular end-diastolic dimension; and FS, fractional shortening. $*P<0.05$.

receptor signal activates CaMKII δ ,²⁷ we treated mActin-Tg mice with the β -blocker bisoprolol to clarify the relationship between β -adrenergic receptor signal and activation of CaMKII δ . The treatment with bisoprolol ameliorated cardiac dysfunction of mActin-Tg mice, and there was no significant difference in cardiac function between wild-type littermates and mActin Tg mice with bisoprolol treatment (Figure VB in the online-only Data Supplement). Furthermore, the increase in CaMKII δ levels in mActin-Tg mice was prevented by bisoprolol treatment (Figure VC in the online-only Data Supplement), suggesting that the activation of CaMKII δ in mActin-Tg mice might be due to activation of β -adrenergic receptor signaling.

To test whether activation of CaMKII δ induces cardiac dysfunction, we first treated mActin-Tg mice with KN-93, a CaMKII inhibitor. Levels of both phosphorylated phospholamban (Thr17) and phospholamban (Ser16) were decreased by KN-93 treatment in mActin-Tg mice (Figure 5B and Figure VD in the online-only Data Supplement). Echocardiography revealed that KN-93 treatment prevented left ventricular dilatation and preserved cardiac function in mActin-Tg mice (Figure 5C). On the other hand, KN-92, an inactive derivative of KN-93, did not show any effects (Figure VE in the online-only Data Supplement). To confirm the role of CaMKII δ in mActin-Tg mice, we crossed mActin-Tg mice and AC3-I mice, which expressed the CaMKII-inhibitory peptide AC3-I in the heart [mActin(+)/AC3-I(+)-DTg].¹⁶ Echocardiography revealed that fractional shortening was better in mActin(+)/AC3-I(+)-DTg mice than in mActin(+)/AC3-I(-)-Tg mice (Figure 5D), suggesting that the activation of CaMKII δ in the DCM mouse model induces left ventricular dilatation and contractile dysfunction.

We next examined the relation between CaMKII δ activation and p53. The increase in p53 was attenuated by treatment with KN-93 or overexpression of AC3-I (Figure 6A and

Figure VIA in the online-only Data Supplement). Furthermore, KN-93 treatment inhibited the increase in Bax expression and TUNEL-positive cardiomyocytes (Figure 6A and 6B). It has been reported that CaMKII δ C, but not CaMKII δ B, induces cardiomyocyte death.^{27–29} To clarify the mechanism of how CaMKII δ increases protein levels of p53 and which

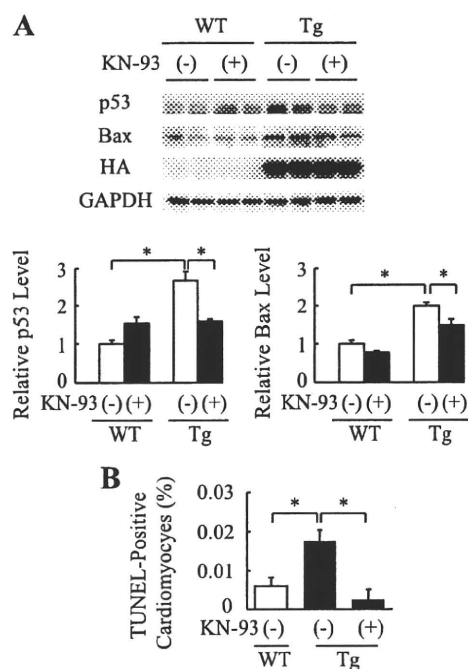


Figure 6. CaMKII δ regulates expression of p53 in cardiomyocytes. **A**, Western blot analyses in the hearts of wild-type littermates (WT) or mActin-Tg (Tg) mice. The graph indicates relative protein levels of p53 or Bax. $n=4$ in each group. $*P<0.05$. **B**, Quantitative analyses of TUNEL-positive cardiomyocytes. $n=5$ in each group. $*P<0.05$.

CaMKII δ , δ B or δ C, plays an important role in apoptosis of cardiomyocytes, we transfected constitutively active forms of CaMKII δ (caCaMKII δ) into cardiomyocytes. Only caCaMKII δ C, not caCaMKII δ B, increased protein levels of p53 (Figure VIB in the online-only Data Supplement). Furthermore, p53 protein levels in caCaMKII δ C-transfected cardiomyocytes did not increase with MG132 treatment compared with MOCK-treated cardiomyocytes (Figure VIC in the online-only Data Supplement). These results suggest that activation of CaMKII δ C increases apoptotic cardiomyocytes at least in part via stabilization of p53 in the DCM mouse model.

Discussion

In the present study, we established a novel mouse model of DCM to clarify the mechanisms of how mutant genes lead to DCM (Table II in the online-only Data Supplement and Figure 1). The mice expressing cardiac α -actin R312H mutant in the heart, which has been reported to cause DCM in humans,⁵ showed dilatation and dysfunction of left ventricle with an increase in ANP messenger RNA levels, which is consistent with human heart failure (Figure 1A and 1E and Table II and Figure III in the online-only Data Supplement). Higher heart rate and hyperphosphorylated phospholamban (Ser16) (Table II in the online-only Data Supplement and Figure 5A) suggest the activation of the sympathetic nervous system to compensate for reduced cardiac systolic function, resulting in an increase in spontaneous Ca²⁺ sparks and Ca²⁺ waves (Table III in the online-only Data Supplement). Myofilament Ca²⁺ sensitivity was decreased in mActin-Tg mice even at 2 months of age (Figure 4B), when cardiac phenotypes such as left ventricular dilatation and cardiac fibrosis were not recognized (Table II in the online-only Data Supplement and Figure 1). These results suggest that the decrease in myofilament Ca²⁺ sensitivity is a primary cause of, not a secondary result from, cardiac dysfunction. Because these phenotypes were quite similar to those of human DCM, mActin-Tg mice are useful for examining the underlying mechanisms of how gene mutations lead to DCM.

There was no significant difference in the peak amplitude of Ca²⁺ transients between wild-type littermates and mActin-Tg mice (Figure IVC in the online-only Data Supplement), suggesting that global Ca²⁺ levels underlying each contractile cycle do not differ between the 2 groups. It has been reported that the peak amplitude of Ca²⁺ transients, which is associated with decreased Ca²⁺ sensitivity and systolic dysfunction, is higher in another mouse model of DCM,⁷ suggesting that Ca²⁺ transients are augmented to compensate for decreased myofilament Ca²⁺ sensitivity in this model. In mActin-Tg mice, despite the preserved Ca²⁺ transients (Figure IVC in the online-only Data Supplement), global cardiac function was gradually impaired (Table II in the online-only Data Supplement). Local Ca²⁺ concentration has been reported to be important for the activation of Ca²⁺-dependent enzymes such as calcineurin, calpain, and CaMKII in cardiomyocytes.³⁰ The activation of these molecules in mActin-Tg mice (Figures 4D, 4E, and 5A) might be attributed to an increase in local Ca²⁺ levels. It still remains to be determined whether local Ca²⁺ levels are really in-

creased and, if so, how the decrease in Ca²⁺ sensitivity increases local Ca²⁺ levels.

Recent reports have shown that CaMKII δ plays a crucial role in cardiovascular diseases.^{16,31} The transgenic mice that overexpressed CaMKII δ showed heart failure with systolic dysfunction and left ventricular dilatation.^{25,26} In this study, CaMKII δ was activated in the hearts of mActin-Tg mice (Figure 5A), and inhibition of CaMKII δ by KN-93 or AC3-I ameliorated cardiac dysfunction in mActin-Tg mice (Figure 5C and 5D), suggesting that CaMKII δ also plays an important role in gene mutation-induced cardiac dysfunction.

It has been reported that apoptosis of cardiomyocytes is observed in hearts of human DCM¹⁰ and that cardiomyocyte death could cause cardiac dysfunction.²⁰ However, it remains unclear whether apoptosis of cardiomyocytes causes cardiac dysfunction and how cardiomyocyte apoptosis is induced in hearts of DCM. In this study, there were more apoptotic cardiomyocytes in mActin-Tg mice (Figure 2A), and cardiac function was improved by protecting cardiomyocytes from apoptosis through overexpression of Bcl-2 (Figure 2B). These results suggest that cardiomyocyte apoptosis plays a crucial role in the development of DCM. Several key proapoptotic and antiapoptotic genes have been reported to be positively or negatively regulated by p53, and increased expression of p53 induces left ventricular dilatation and dysfunction in mice deficient in MDM4, an E3 ligase for p53.²³ Furthermore, we have recently demonstrated that p53 is critically involved in pressure overload-induced cardiac dysfunction.²² The protein levels of p53 were increased in mActin-Tg mice (Figure 3A), and loss of a single p53 allele reduced the number of apoptotic cardiomyocytes (Figure 3D) and improved cardiac function (Figure 3B). These results suggest that p53 is critically involved in induction of cardiomyocyte apoptosis, resulting in left ventricular dysfunction in the mouse model of DCM.

The present study indicates that p53 might be a therapeutic target for DCM. In this study, CaMKII δ was activated in the hearts of mActin-Tg mice (Figure 5A), and the inhibition of CaMKII δ attenuated the increase in p53 protein levels (Figure 6A and Figure VIA in the online-only Data Supplement), suggesting that CaMKII δ regulates protein levels of p53 in the DCM model mice. Although it remains to be determined how CaMKII δ regulates protein levels of p53, inhibition of CaMKII δ may become a new therapeutic strategy for DCM patients by reducing p53 protein levels in the heart.

Limitations

This study has a couple limitations. First, we cannot completely rule out the nonspecific effects of overexpression of cardiac α -actin gene with tag because of a lack of transgenic mice that overexpress wild-type cardiac α -actin gene. However, we think the cardiac dysfunction observed in mActin-Tg was due to cardiac expressions of the cardiac α -actin R312H mutant in the heart, not to high-level expressions of the cardiac α -actin protein with tag because of the following reasons: We obtained 3 independent founders of the transgenic mice, and the reduction in cardiac function was well correlated with protein levels of the cardiac α -actin R312H mutant (Figure I in the online-only Data Supplement). An-

other transgenic mouse that expressed cardiac α -actin A331P mutant with an HA tag in the heart did not show cardiac dysfunction (Table I in the online-only Data Supplement), although the protein levels of the mutant in the A331P mutant transgenic mice were almost same as those of the R312H mutant in line 307, which had the highest expression (Figure II in the online-only Data Supplement). Second, we found that CaMKII δ C increases p53 protein levels mainly by its stabilization, but the underlying mechanisms remain to be determined.

Acknowledgments

We thank J. Robbins (Children's Hospital Research Foundation, Cincinnati, Ohio) for a fragment of α -myosin heavy chain gene promoter, J.D. Molkentin (Children's Hospital Research Foundation, Cincinnati, Ohio) for NFAT-luciferase reporter transgenic mice, M.D. Schneider (Imperial College, London, UK) for Bcl-2 transgenic mice, and E.N. Olson (UT Southwestern Medical Center, Dallas, Tex) for constitutively active forms of CaMKII δ . We thank E. Fujita, R. Kobayashi, Y. Ishiyama, M. Ikeda, I. Sakamoto, A. Furuyama, and Y. Ohtsuki for technical support, as well as M. Iiyama, K. Matsumoto, Y. Ishikawa, and Y. Yasukawa for animal care.

Sources of Funding

This work was supported by a Grant-in-Aid for Scientific Research on Priority Areas (to Dr Komuro) and a Grant-in-Aid for Scientific Research (C) (20590857 to Dr Oka) from the Ministry of Education, Culture, Sports, Science and Technology; the Japan Heart Foundation/Novartis Grant for Research Award on Molecular and Cellular Cardiology; Japan Foundation for Applied Enzymology; Suzuken Memorial Foundation; and Mitsubishi Pharma Research Foundation (to Dr Toko). This work was supported by National Institutes of Health grants R01 HL079031, R01 HL070250, and R01 HL096652 and by the Fondation Leducq Award to the Alliance for Calmodulin Kinase Signaling in Heart Disease (to Dr Anderson).

Disclosures

Dr Anderson is named on patents claiming to treat heart failure by CaMKII inhibition and is a cofounder of Allosteros. The other authors report no conflicts.

References

- Michels VV, Moll PP, Miller FA, Tajik AJ, Chu JS, Driscoll DJ, Burnett JC, Rodeheffer RJ, Chesebro JH, Tazelaar HD. The frequency of familial dilated cardiomyopathy in a series of patients with idiopathic dilated cardiomyopathy. *N Engl J Med*. 1992;326:77–82.
- Maron BJ, Towbin JA, Thiene G, Antzelevitch C, Corrado D, Arnett D, Moss AJ, Seidman CE, Young JB. Contemporary definitions and classification of the cardiomyopathies: an American Heart Association scientific statement from the Council on Clinical Cardiology, Heart Failure and Transplantation Committee; Quality of Care and Outcomes Research and Functional Genomics and Translational Biology Interdisciplinary Working Groups; and Council on Epidemiology and Prevention. *Circulation*. 2006;113:1807–1816.
- Ahmad F, Seidman JG, Seidman CE. The genetic basis for cardiac remodeling. *Annu Rev Genomics Hum Genet*. 2005;6:185–216.
- Knoll R, Hoshijima M, Hoffman HM, Person V, Lorenzen-Schmidt I, Bang ML, Hayashi T, Shiga N, Yasukawa H, Schaper W, McKenna W, Yokoyama M, Schork NJ, Omens JH, McCulloch AD, Kimura A, Gregorio CC, Poller W, Schaper J, Schultheiss HP, Chien KR. The cardiac mechanical stretch sensor machinery involves a Z disc complex that is defective in a subset of human dilated cardiomyopathy. *Cell*. 2002;111:943–955.
- Olson TM, Michels VV, Thibodeau SN, Tai YS, Keating MT. Actin mutations in dilated cardiomyopathy, a heritable form of heart failure. *Science*. 1998;280:750–752.
- Towbin JA, Bowles NE. Genetic abnormalities responsible for dilated cardiomyopathy. *Curr Cardiol Rep*. 2000;2:475–480.
- Du CK, Morimoto S, Nishii K, Minakami R, Ohta M, Tadano N, Lu QW, Wang YY, Zhan DY, Mochizuki M, Kita S, Miwa Y, Takahashi-Yanaga F, Iwamoto T, Ohtsuki I, Sasaguri T. Knock-in mouse model of dilated cardiomyopathy caused by troponin mutation. *Circ Res*. 2007;101:185–194.
- Kawada T, Masui F, Tezuka A, Ebisawa T, Kumagai H, Nakazawa M, Toyo-Oka T. A novel scheme of dystrophin disruption for the progression of advanced heart failure. *Biochim Biophys Acta*. 2005;1751:73–81.
- Kyoi S, Otani H, Matsuhisa S, Akita Y, Tatsumi K, Enoki C, Fujiwara H, Imamura H, Kamihata H, Iwasaka T. Opposing effect of p38 MAP kinase and JNK inhibitors on the development of heart failure in the cardiomyopathic hamster. *Cardiovasc Res*. 2006;69:888–898.
- Olivetti G, Abbi R, Quaini F, Kajstura J, Cheng W, Nitahara JA, Quaini E, Di Loreto C, Beltrami CA, Krajewski S, Reed JC, Anversa P. Apoptosis in the failing human heart. *N Engl J Med*. 1997;336:1131–1141.
- Bulfield G, Siller WG, Wight PA, Moore KJ. X chromosome-linked muscular dystrophy (mdx) in the mouse. *Proc Natl Acad Sci U S A*. 1984;81:1189–1192.
- Cooper BJ, Winand NJ, Stedman H, Valentine BA, Hoffman EP, Kunkel LM, Scott MO, Fischbeck KH, Kornegay JN, Avery RJ, Williams JR, Schmickel RD, Sylvester JE. The homologue of the Duchenne locus is defective in X-linked muscular dystrophy of dogs. *Nature*. 1988;334:154–156.
- Nigro V, Okazaki Y, Belsito A, Piluso G, Matsuda Y, Politano L, Nigro G, Ventura C, Abbondanza C, Molinari AM, Acampora D, Nishimura M, Hayashizaki Y, Puca GA. Identification of the Syrian hamster cardiomyopathy gene. *Hum Mol Genet*. 1997;6:601–607.
- Tanaka M, Nakae S, Terry RD, Mokhtari GK, Gunawan F, Balsam LB, Kaneda H, Kofidis T, Tsao PS, Robbins RC. Cardiomyocyte-specific Bcl-2 overexpression attenuates ischemia-reperfusion injury, immune response during acute rejection, and graft coronary artery disease. *Blood*. 2004;104:3789–3796.
- Wilkins BJ, Dai YS, Bueno OF, Parsons SA, Xu J, Plank DM, Jones F, Kimball TR, Molkentin JD. Calcineurin/NFAT coupling participates in pathological, but not physiological, cardiac hypertrophy. *Circ Res*. 2004;94:110–118.
- Zhang R, Khoo MS, Wu Y, Yang Y, Grueter CE, Ni G, Price EE Jr, Thiel W, Guatimosim S, Song LS, Madu EC, Shah AN, Vishnivetskaya TA, Atkinson JB, Gurevich VV, Salama G, Lederer WJ, Colbran RJ, Anderson ME. Calmodulin kinase II inhibition protects against structural heart disease. *Nat Med*. 2005;11:409–417.
- Donehower LA, Harvey M, Slagle BL, McArthur MJ, Montgomery CA Jr, Butel JS, Bradley A. Mice deficient for p53 are developmentally normal but susceptible to spontaneous tumours. *Nature*. 1992;356:215–221.
- VanGuilder HD, Vrana KE, Freeman WM. Twenty-five years of quantitative PCR for gene expression analysis. *Biotechniques*. 2008;44:619–626.
- Olson TM, Doan TP, Kishimoto NY, Whitby FG, Ackerman MJ, Fananapazir L. Inherited and de novo mutations in the cardiac actin gene cause hypertrophic cardiomyopathy. *J Mol Cell Cardiol*. 2000;32:1687–1694.
- Wencker D, Chandra M, Nguyen K, Miao W, Garantziotis S, Factor SM, Shirani J, Armstrong RC, Kitsis RN. A mechanistic role for cardiac myocyte apoptosis in heart failure. *J Clin Invest*. 2003;111:1497–1504.
- Ryan KM, Phillips AC, Vousden KH. Regulation and function of the p53 tumor suppressor protein. *Curr Opin Cell Biol*. 2001;13:332–337.
- Sano M, Minamino T, Toko H, Miyauchi H, Orimo M, Qin Y, Akazawa H, Tateno K, Kayama Y, Harada M, Shimizu I, Asahara T, Hamada H, Tomita S, Molkentin JD, Zou Y, Komuro I. p53-induced inhibition of Hif-1 causes cardiac dysfunction during pressure overload. *Nature*. 2007;446:444–448.
- Xiong S, Van Pelt CS, Elizondo-Fraire AC, Fernandez-Garcia B, Lozano G. Loss of Mdm4 results in p53-dependent dilated cardiomyopathy. *Circulation*. 2007;115:2925–2930.
- Hoch B, Meyer R, Hetzer R, Krause EG, Karczewski P. Identification and expression of delta-isoforms of the multifunctional Ca²⁺/calmodulin-dependent protein kinase in failing and nonfailing human myocardium. *Circ Res*. 1999;84:713–721.
- Zhang T, Johnson EN, Gu Y, Morissette MR, Sah VP, Gigena MS, Belke DD, Dillmann WH, Rogers TB, Schulman H, Ross J Jr, Brown JH. The cardiac-specific nuclear delta(B) isoform of Ca²⁺/calmodulin-dependent protein kinase II induces hypertrophy and dilated cardiomyopathy associated with increased protein phosphatase 2A activity. *J Biol Chem*. 2002;277:1261–1267.

26. Zhang T, Maier LS, Dalton ND, Miyamoto S, Ross J Jr, Bers DM, Brown JH. The deltaC isoform of CaMKII is activated in cardiac hypertrophy and induces dilated cardiomyopathy and heart failure. *Circ Res.* 2003;92:912-919.
27. Zhu WZ, Wang SQ, Chakir K, Yang D, Zhang T, Brown JH, Devic E, Kobilka BK, Cheng H, Xiao RP. Linkage of beta1-adrenergic stimulation to apoptotic heart cell death through protein kinase A-independent activation of Ca²⁺/calmodulin kinase II. *J Clin Invest.* 2003;111:617-625.
28. Peng W, Zhang Y, Zheng M, Cheng H, Zhu W, Cao CM, Xiao RP. Cardioprotection by CaMKII-deltaB is mediated by phosphorylation of heat shock factor 1 and subsequent expression of inducible heat shock protein 70. *Circ Res.* 2010;106:102-110.
29. Zhu W, Woo AY, Yang D, Cheng H, Crow MT, Xiao RP. Activation of CaMKIIdeltaC is a common intermediate of diverse death stimulus-induced heart muscle cell apoptosis. *J Biol Chem.* 2007;282:10833-10839.
30. Wu X, Zhang T, Bossuyt J, Li X, McKinsey TA, Dedman JR, Olson EN, Chen J, Brown JH, Bers DM. Local InsP₃-dependent perinuclear Ca²⁺ signaling in cardiac myocyte excitation-transcription coupling. *J Clin Invest.* 2006;116:675-682.
31. Ling H, Zhang T, Pereira L, Means CK, Cheng H, Gu Y, Dalton ND, Peterson KL, Chen J, Bers D, Heller Brown J. Requirement for Ca²⁺/calmodulin-dependent kinase II in the transition from pressure overload-induced cardiac hypertrophy to heart failure in mice. *J Clin Invest.* 2009;119:1230-1240.

CLINICAL PERSPECTIVE

Heart failure is an important cause of morbidity and mortality in many industrial countries, and dilated cardiomyopathy (DCM) is one of its major causes. Molecular genetic studies over the last 2 decades have revealed many mutations of various genes in DCM patients, but the precise mechanisms of how such mutations lead to DCM remain largely unknown partly because of a lack of good animal models of DCM. Here, we established the mouse model of DCM by expressing a mutated cardiac α -actin gene, which has been reported in patients with DCM, in the heart. The transgenic mice showed gradual dilatation and dysfunction of the left ventricle, resulting in death by heart failure. These phenotypes of the transgenic mice were quite similar to those of human DCM. The number of apoptotic cardiomyocytes and protein levels of p53 were increased in the hearts of the DCM mice. Overexpression of Bcl-2, an antiapoptotic factor, or downregulation of p53 decreased the number of apoptotic cardiomyocytes and improved cardiac function. The DCM mice showed activation of CaMKII δ . The inhibition of CaMKII δ prevented the increase in p53 and apoptotic cardiomyocytes and ameliorated cardiac function. These results suggest that CaMKII δ plays a critical role in the development of heart failure in part by accumulation of p53 and induction of cardiomyocyte apoptosis in the DCM mouse model. The inhibition of CaMKII δ may become a new therapeutic strategy for DCM patients.

6

心臓移植

中谷武嗣

● 心臓移植の歴史

末期心不全に対する心臓置換療法として、心臓移植と人工心臓の研究が行われ、心臓移植は1967年に南アフリカにおいてBarnardがはじめて施行し、全置換型人工心臓は、1969年に心臓移植へのつなぎ（ブリッジ）として米国においてD. A. Cooleyが始めて用いた。1960年代後半にはわが国で実施された1例も含め多くの国で行われ、100例以上の心臓移植が実施されたが多数の患者が数ヶ月以内に死亡したため、1970年代は限られた施設でのみ研究が続けられた。その中で、経静脈的心筋生検法が開発されるとともに拒絶反応の病理学的診断基準が検討され、また新たな免疫抑制剤としてciclosporinが導入されたことにより、心臓移植の成績は向上した。1980年代初頭からは欧米において末期心不全に対する治療選択として受け入れられるようになり、1990年代前半には国際レジストリーで年間4,000例以上に実施された¹⁾。わが国では、1968年実施以降長年にわたり臓器移植に対する不信感が強く、1997年10月16日に「臓器の移植に関する法律」が施行され、脳死臓器移植が行われる体制となった。そして、1999年2月にこの法律による脳死下での臓器提供が行われ、心臓移植が実施された。その後、2001年5月からは拡張型心筋症（DCM）および拡張相肥大型心筋症（D-HCM）に対する心臓移植手術が高度先進医療として承認され、2006年4月からは健康保険において同種心移植術として移植関係学会合同委員会で心臓移植実施施設として選定された施設での実施が認められ、これまでに64例の心臓移植が行われた²⁾。

Topics

抗体関連型拒絶反応

拒絶反応には、細胞性免疫による急性拒絶反応とともに液性免疫による抗体関連型拒絶反応がある。特に移植直後に発生する超急性拒絶反応は、前感作抗体によるものである。このため、わが国では、レシピエント選択において、ドナーに対する前感作抗体を検査し、陽性例は除外するようになっている。しかし、わが国のレシピエントは大多数がLVAS装置例であり、手術時などに多量の輸血が行われており、抗HLA抗体を有している例が多い。このように自己以外のHLAに感作された心臓移植待機患者においては、移植後の免疫抑制に注意が必要で、心筋生検検査においても免疫染色を行う必要がある。また、われわれは1999年施行の第1例目から、paner reactive antibody (PRA) 検査により患者の抗HLA抗体の検査を行い、病理検査も含めた病態に応じて血漿交換、グロブリン製剤投与、免疫抑制剤の調整などを行ってきた。このような感作された移植待機患者への対応は、日本組織適合性学会および日本移植学会でも検討されてきた。心臓移植待機患者においてもこれまで種々の検討がなされてきたが、LVASによるブリッジ例が増加していることもあり、心臓移植前あるいは移植後の対応、病理診断基準の確立などの必要性が国際心肺移植学会で取り上げられ、2008年4月にコンセンサス会議が開催され、以後も検討が続けられている。

Kobashigawa J et al : Report from a consensus conference on the sensitized patient awaiting heart transplantation. J Heart Lung Transplant 28 : 123-125, 2009

● 心臓移植の適応

わが国における適応基準を表1に示す。主な適応疾患はDCMおよびD-HCMと虚血性心筋疾患でDCMおよびD-HCMでは心筋生検による確定診断が必須である。心臓移植後は一生にわたる免疫抑制療法が必要であり、適応判定において移植以外の治療手段、予測される余命、移植後の治療に対するコンプライアンスなど表1の2、3で示す適応条件および除外条件を慎重に検討する。

表 1 心臓移植におけるレシピエント適応基準

<p>1. 適応となる疾患</p> <p>心臓移植の適応となる疾患は、従来の治療法では救命ないし延命の期待がもてない以下の重症心疾患とする。</p> <p>a. 拡張型心筋症、および拡張相の肥大型心筋症</p> <p>b. 虚血性心筋疾患</p> <p>c. その他（日本循環器学会および日本小児循環器学会の心臓移植適応検討会で承認する心臓疾患）</p>
<p>2. 適応条件</p> <p>a. 不治の末期的状態にあり、以下のいずれかの条件を満たす場合</p> <p>1) 長期間またはくり返し入院治療を必要とする心不全</p> <p>2) β遮断薬および ACE 阻害薬を含む従来の治療法では NYHA III 度ないし IV 度から改善しない心不全</p> <p>3) 現存するいかなる治療法でも無効な致死的重症不整脈を有する症例</p> <p>b. 年齢は 60 歳未満が望ましい</p> <p>c. 本人および家族の心臓移植に対する十分な理解と協力が得られること</p>
<p>3. 除外条件</p> <p><絶対的除外条件></p> <p>a. 肝臓、腎臓の不可逆的機能障害</p> <p>b. 活動性感染症（サイトメガロウイルス感染症を含む）</p> <p>c. 肺高血圧症（肺血管抵抗が血管拡張薬を使用しても 6 wood 単位以上）</p> <p>d. 薬物依存症（アルコール性心筋疾患を含む）</p> <p>e. 悪性腫瘍</p> <p>f. HIV 抗体陽性</p> <p><相対的除外条件></p> <p>a. 腎機能障害、肝機能障害</p> <p>b. 活動性消化性潰瘍</p> <p>c. インスリン依存性糖尿病</p> <p>d. 精神神経症（自分の病氣、病態に対する不安を取り除く努力をしても、何ら改善がみられない場合に除外条件となることがある）</p> <p>e. 肺梗塞症の既往、肺血管閉塞病変</p> <p>f. 膠原病などの全身性疾患</p>

● 適応決定と心臓移植待機中の管理

現在、わが国での適応決定は、各施設内適応検討会に加え日本循環器学会心臓移植委員会適応検討小委員会の 2 段階審査で行なわれる。適応ありと判定されれば IC を含む諸手続きを行い、日本臓器移植ネットワークに登録し移植待機となる。これまでに 376 例が登録され、現在 139 例が待機中である。なお、現在わが国での心臓移植施設は移植関係学会合同委員会で選定された 6 施設（国立循環器病センター、大阪大学、東京大学、東京女子医科大学、九州大学、東北大学）に限定されて

いる。

移植待機中も心不全治療を続け、心不全が進行し重要臓器の機能障害を伴うようになる場合は、心臓移植へのつなぎとして左心補助人工心臓（left ventricular assist system: LVAS）の適応を考慮する。わが国では、多くの症例で申請時あるいは待機中に LVAS が適応されている。現時点では、体外設置型 LVAS の東洋紡製国立循環器病センター型のみが保険適応で、数種の植込み型 LVAS の治療あるいは承認申請が行われている。待機中に心機能が改善し移植対象外となる症例や、あるいは感染や臓器障害などにより適応から外れる症例があるため、適宜再検討を行なう。

● ドナー心の評価とレシピエント候補の決定

臓器移植のドナーとして、全身性の活動性感染症、HIV 抗体・HTLV-1 抗体・HBs 抗原・HCV 抗体などの陽性者、クロイツフェルト・ヤコブ病およびその疑い、悪性腫瘍などがなければ検討される。また、心疾患、心臓外傷、開心術の既往があれば適さない。心臓移植のドナーとしては 60 歳以下が対象となるが、男性 45 歳、女性 50 歳以上では冠状動脈硬化性病変の検討が必要である。心電図や心エコー図などで心機能を検討するが、大量（dopamine 10 μ g/kg/分相当以上）のカテコラミンが用いられている場合は慎重に検討する。最終判定は、ドナー手術において開胸下に冠動脈病変を含め触診および視診により行う。

レシピエント候補は、日本臓器移植ネットワーク登録中の待機リストから選定される。適合条件として、血液型の一致あるいは適合、サイズの適合（体重差 -20~+30% が望ましい）、前感作抗体がないこと（リンパ球・クロスマッチを実施）がある。これら適合条件に合致する候補者が複数いる場合は、虚血許容時間（4 時間以内に血流再開ができること）、医学的緊急度（VAS, IABP, 人工呼吸あるいは重症室管理で持続的強心薬投与を必要とする場合が緊急度の高い status 1 とする）、ABO 式血液型および待機期間により優先順位を決定する。status 1 を優先し、複数の同一条件候補がいる場合は待機期間の長い者から優先される。

● 心臓移植手術

ドナー情報は予測できないため、常に短時間で準備ができる体制が必要である。また、心臓は他の臓器よりも許容虚血時間が短いため、ドナーチームとレシピエントチームの緊密な連係が重要である。ドナー手術において、直接視診および触診により最終的なドナー心の評価を行う。

レシピエント手術法には、心房位吻合を行なう Lower-Shumway 法、上・下大静脈で吻合する bicaval 法、およびレシピエントの右房後壁の一部を温存して上・下大静脈で吻合する modified bicaval 法がある。現在わが国では modified bicaval 法が多く用いられている。

● 心臓移植後の管理

心臓移植後の管理においては、移植心不全、拒絶反応、感染症、悪性腫瘍、冠動脈病変に注意する必要がある。

1 移植心不全

ドナー心への強心薬の使用状況と心機能、心保存法、手術手技などが関係する。ドナー心機能評価および心保存を確実に行うとともに、虚血時間の短縮が重要で、心保存液として我々は Celsior 液を用いている。また、搬送では、小型ジェット機やヘリコプターの活用が必要となる。

2 急性拒絶反応と免疫抑制療法

心臓移植では、拒絶反応の診断は定期的な内頸静脈からの心内膜心筋生検法により行われ、国際心臓肺移植学会の基準により判定される。拒絶反応は、特異的な臨床症状や所見がないため、心筋生検による定期的な病理的診断が必要である。我々は、移植後3週は毎週、その後5週、7週ついで11週に行い、その後4.5ヵ月、6ヵ月、9ヵ月、12ヵ月に実施し、以降は半年ごとに数年間行い、安定している場合には1回/年としている。病理診断は原則、心筋生検施行日に行い、HE染色とMasson-Trichrome染色により国際心臓肺移植学会の病理診断基準に従って診断する。

免疫抑制療法は、カリシニューリン阻害薬である ciclosporin あるいは tacrolimus、核酸合成阻害薬

である mycophenolate mofetil、およびステロイド薬 prednisolone の三剤併用療法が行われる。

われわれは、術中にステロイドとして methylprednisolone を麻酔導入後およびドナー心への血流再開直前に500mg 静注している。

その後ステロイドについては、MP 125mg 8時間ごとから開始し、徐々に減量し、PRDとして、1~1.5ヵ月後に0.1mg/kg/日への減量を目指している。また、6ヵ月以降拒絶反応なければステロイド中止を試みている。

カリシニューリン阻害薬としては、症例により ciclosporin あるいは tacrolimus を用いている。ciclosporin では、TDMによりC0、C2、およびAUC 0~4により投与量を調整している。tacrolimus では、trough値で投与量を調整し、6ヵ月までは12~15ng/mL、12ヵ月までは10~12ng/mL、以降は8ng/mL程度を目標としている。

MMFに関しては、2ないし3g/日の投与を行い、白血球数が4,000/mm³以下に低下した場合には投与量を調整している。また、検査入院時にAUC 0~12を測定し、39.25μg/mL以上を目標として投与量を調整している。

治療が必要な拒絶反応を認めた場合にまずステロイドパルス療法を行い、パルス療法に抵抗性の場合には抗胸腺抗体による治療を行う。

また、抗体関連型拒絶反応への配慮も必要であり、移植後早期には心筋生検検査において免疫染色も追加している。治療が必要な場合には、血漿交換、グロブリン製剤の投与を行う。

3 移植後冠動脈病変

慢性拒絶反応と呼ばれてきたが、移植心冠動脈にびまん性の求心性内膜肥厚が進行する。ドナー心は徐神経されているため虚血に対して胸痛を自覚せず、突然心原性ショックを発症したり、不整脈による突然死を引き起こすことがある。このため、冠動脈造影と血管内超音波検査(IVUS)を定期的に行う。我々は、移植後3ヵ月でドナー心の冠動脈の評価を行い、以後1年後の心筋生検時に同時に行っている。

この移植後冠動脈病変は心臓移植後の長期予後に大きく影響しており、危険因子には、免疫関連として、T細胞の活性化、細胞性拒絶反応、細胞増殖、HLAミスマッチなど、その他の因子とし